Advances in Aircraft and Spacecraft Science, *Vol. 5, No. 1 (2018) 21-49*
DOI: https://doi.org/10.12989/aas.2018.5.1.021

Geometrical nonlinear bending characteristics of SWCNTRC doubly curved shell panels

Shivaji G. Chavan* and Achchhe Lal[a]

Department of Mechanical Engineering, S.V.N.I.T, Surat, Gujarat 395007, India

(Received March 7, 2017, Revised May 8, 2017, Accepted September 5, 2017)

Abstract. In this paper, geometric nonlinear bending characteristics of single wall carbon nanotube reinforced composite (SWCNTRC) doubly curved shell panels subjected to uniform transversely loadings are investigated. The nonlinear mathematical model is developed for doubly curved SWCNTRC shell panel on the basis of higher-order shear deformation theory and Green– Lagrange nonlinearity. All nonlinear higher order terms are included in the mathematical model. The effective material properties of SWCNTRC are estimated by using Eshelby-Mori-Tanaka micromechanical approach. The governing equation of the shell panel is obtained using the total potential energy principle and a Newton-Raphson iterative method is employed to compute the nonlinear displacement and stresses. The present results are compared with published literature. The effect of SWCNT volume fraction, width-to-thickness ratio, radius-to-width ratio (R/a), boundary condition, linear and nonlinear deflection, stresses and different types of shell geometry on nonlinear bending response is investigated.

Keywords: SWCNTRC shell panel; micromechanics; nonlinear bending; green-lagrange nonlinearity; HSDT; newton-raphson method

1. Introduction

Wide application of reinforced composite shells in mechanical, civil, aeronautical, automotive, biomedical, nuclear, petro-chemical and marine engineering has created the necessity of the analysis of their responses precisely. It is well known that the shell structures are much stronger and stiffer than other structural forms due to their geometrical form (three-dimensional curvatures). Some researchers are reported in literature review as follow: Lal *et al.* (2011) investigated nonlinear bending response of laminated composite spherical shell panel with system randomness subjected to hygro-thermo-mechanical loading. Sadowski and Michael (2013) presented solid continuum finite elements and shell finite elements in the modeling of the nonlinear plastic buckling behavior of cylindrical shells. Jin *et al.* (2013) reported vibration analysis of moderately thick composite laminated cylindrical shells with arbitrary boundary conditions. Song *et al.* (2016) expressed nonlinear vibration analysis of CNT-reinforced

*Corresponding author, Ph.D.
E-mail: shivajigchavan@gmail.com
[a]Assistant Professor

http://www.techno-press.org/?journal=aas&subpage=7 ISSN: 2287-528X (Print), 2287-5271 (Online)

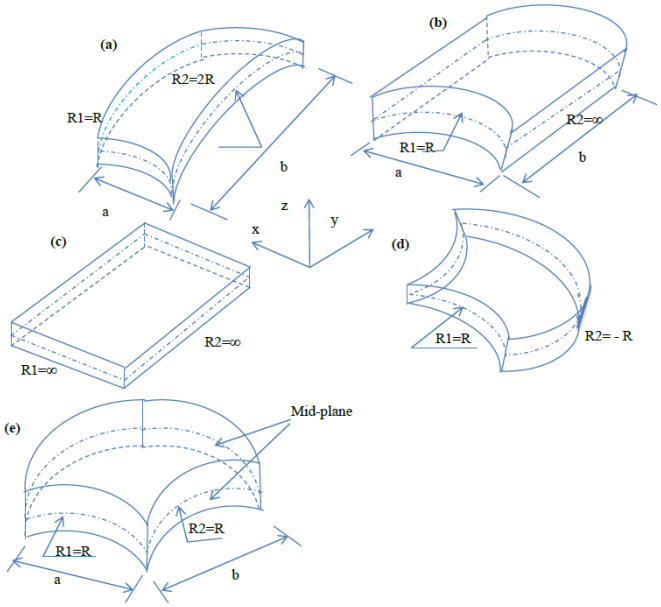

Fig. 1 single and doubly curved SWCNTRC-shell panels (a) Elliptical, (b) Cylindrical, (c) Flat, (d) Hyperbolic, (e) Spherical

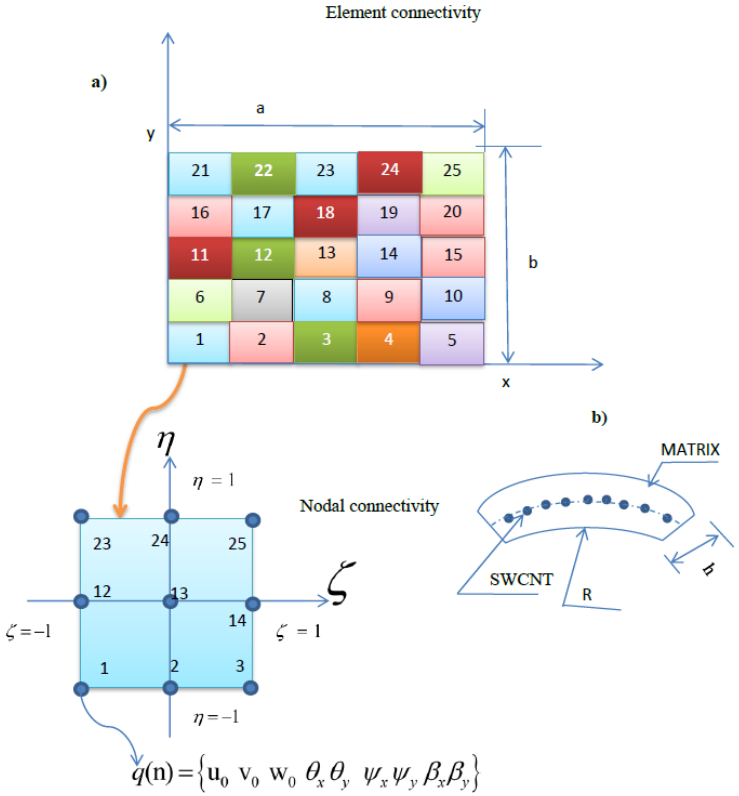

Fig 2(a) SWCNTRC shell discritized using lagrange qudratic isopramrtic nine noded element, (b) Uniformaly Dicstributed SWCNTRC shell panels

functionally graded composite cylindrical shells in thermal environments. Shen and Xiang (2014) reported on nonlinear bending of nanotube-reinforced composite cylindrical panels resting on elastic foundations in thermal environments. Kar and Panda (2015) investigated thermoplastic analysis of functionally graded doubly curved shell panels using nonlinear finite element method. They developed nonlinear mathematical model of doubly curved shell panel based on higher-order shear deformation theory and Green-Lagrange geometric nonlinearity. Lopatin *et al.* (2016) studied bending of the composite lattice cylindrical shell with the mid-span rigid disk loaded by transverse inertia forces. Sofiyev *et al.* (2017) presented nonlinear vibration of composite orthotropic cylindrical shells on the non-linear elastic foundations within the shear deformation theory. Singh and Panda (2014) analyzed nonlinear free vibration analysis of single/doubly curved composite shallow shell panels. Panda and singh (2009) presented nonlinear free vibration of spherical shell panel using higher order shear deformation theory. Tornabene and Viola (2009) investigated free vibration analysis of functionally graded panels and shells, they used First order Shear Deformation Theory (FSDT) to study of moderately thick structural elements analysis. Orakdogen *et al.* (2010) reported Finite element analysis of functionally graded plates for coupling effect of extension and bending. Shariyat (2012) presented a general nonlinear global-local theory for bending and buckling analyses of imperfect cylindrical laminated and sandwich shells under thermo-mechanical load. Dai and Ting (2014) presented for the thermo-elastic bending of a functionally graded material cylindrical shell subjected to a uniform transverse mechanical load and non-uniform thermal load. Lezgy-Nazargah and Cheraghi (2015) investigated an exact Peano Series solution for bending analysis of imperfect layered FG neutral magneto-electro- elastic plates resting on elastic foundations. The free vibration and the bending behavior of carbon nanotube reinforced composite plate by using three different shear deformation theories under thermal environment were presented by Mehar and Panda (2016) Mahapatra *et al.* (2017) investigated The flexural behavior of the functionally graded sandwich spherical panel under uniform thermal environment. Katariya and Panda (2016) develop mathematical model for laminated curved structure of different geometries using higher -order shear deformation theory to evaluate in-plane and out of plane shear stress and strains correctly, Mehar *et al.* (2015) studied the free vibration behavior of functionally graded carbon nanotube reinforced composite plate under elevated thermal environment. The nonlinear free vibration behaviour of functionally graded carbon nanotube reinforced composite flat panel in temperature dependent material properties for different grading were investigated by Mehar and Panda (2016). Mehar and Panda (2016) presented the geometrical nonlinear static behaviour of the functionally graded carbon nanotube reinforced doubly curved shell panel under uniform thermal environment. The nonlinear static deflections of a functionally graded carbon nanotube (FG-CNT) reinforced flat composite panel under a uniform thermal environment for different end conditions were examined by Mehar and Panda (2016). Mehar and Panda (2016) investigated the vibration characteristics of carbon nanotube reinforced sandwich curved shell panel under the elevated thermal environment. Kulikov *et al.* (2016) investigated exact geometry solid-shell element based on a sampling surfaces technique for 3D stress analysis of doubly-curved composite shells. Chavan and Lal (2017) presented bending analysis of nanocomposite plate subjected to unform pressure. Khatibinia Mohsen *et al.* (2016) presented a layered approach to the non-linear static and dynamic analysis of rectangular reinforced concrete slabs. Shariq *et al.* (2017) studied effect of the experimental investigation of effect on time dependent deflection of reinforced beam due to creep and shrinkage.

The nonlinear mathematical model of doubly curved SWCNTRC shell panel is developed based on HSDT and Green-Lagrange nonlinearity. The nonlinear higher order terms are included

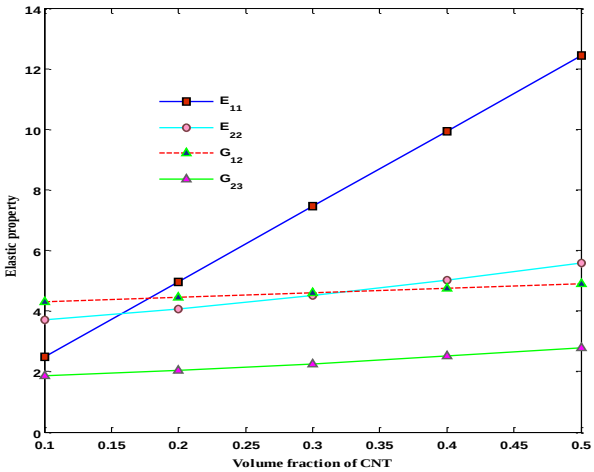

Fig. 3 The effect of Elastic properties on increasing volume fraction of SWCNT

in the mathematical model. The effective material properties of SWCNTRC are estimated by using Eshelby-Mori-Tanaka micromechanical approach. A Newton-Raphson iterative method is used to compute the nonlinear bending responses. The proposed numerical analysis has been validated with available literature. Numerical simulations are carried out to investigate effect of various parameters on geometric nonlinear behaviors of SWCNTRC shell panels. The effect of SWCNT volume fraction, width-to-thickness ratio, radius-to-width ratio (R/a), boundary condition, linear and nonlinear deflection, stresses and different types of shell geometry on nonlinear bending response of SWCNTRC shell panels is investigated.

2. Micromechanics approach

In this section the Mori-Tanaka's method to the computation of the effective properties of SWCNTR composites. it is assumed that Nano-composite reinforced by straight and long CNT fibers, also the fibers are uniformly distributed in the isotropic Matrix of composite as shown in Fig. 2(b). The effective elastic modulus of SWCNT can be defined as, (Aragh *et al.* 2012, Chavan and Lal 2017)

$$k = \frac{E_m\left\{E_m V_m + 2k_{CNT}(1+\nu_m)[1+V_{CNT}(1-2\nu_m)]\right\}}{2(1+\nu_m)[E_m(1+V_{CNT}-2\nu_m)+2V_m k_{CNT}(1-\nu_m-2\nu_m^2)]} \tag{1}$$

$$l = \frac{E_m\left\{V_m\nu_m[E_m+2k_{CNT}(1+\nu_m)]+2V_{CNT}l_{CNT}(1-\nu_m^2)\right\}}{(1+\nu_m)[E_m(1+V_{CNT}-2\nu_m)+2V_m k_{CNT}(1-\nu_m-2\nu_m^2)]} \tag{2}$$

$$n = \frac{E_m^2 V_m(1+V_{CNT}-V_m\nu_m)+2V_m\nu_{CNT}(k_{CNT}n_{CNT}-l_{CNT}^2)(1-2\nu_m)}{(1+\nu_m)[E_m(1+V_{CNT}-2\nu_m)+2V_m k_{CNT}(1-\nu_m-2\nu_m^2)]} \tag{3}$$

$$+\frac{E_m[2V_m^2k_{CNT}(1-\nu_m)+V_{CNT}n_{CNT}(1-2\nu_m+V_{CNT})-42V_ml_{CNT}\nu_m]}{2V_mk_{CNT}(1-\nu_m+\nu_m^2)+E_m(1-V_{CNT}+2\nu_m)}$$

$$p=\frac{E_m[E_mV_m+2(1+V_{CNT})p_{CNT}(1+\nu_m)]}{2(1+\nu_m)[E_m(1+V_{CNT})+2V_mp_{CNT}(1+\nu_m)]} \tag{4}$$

$$m=\frac{E_m[E_mV_m+2m_{CNT}(1+\nu_m)(3+V_{CNT}-4\nu_m)}{2(1+\nu_m)\{E_m[(V_m+4V_{CNT}(1-\nu_m)]+2V_mm_{CNT}(3-\nu_m-4\nu_m^2)]\}} \tag{5}$$

The effect of the volume fractions of SWCNT on elastic property of SWCNTRC shell panel are plotted in Fig. 3.

The overall composite properties of SWCNTRC shell panels can be estimated by,

$$E_{11}=n-\frac{l^2}{k};\quad E_{22}=\frac{4m(kn-l^2)}{kn-l^2+mn};\quad G_{12}=2p;\nu_{12}=\frac{l}{2k}. \tag{6}$$

3. Mathematical formulation

3.1 displacement field

A different geometry of SWCNTRC shell panels are shown in Fig. 1. The following displacement field for the SWCNTRC shell panels based on the HSDT is given by (Kar and Panda 2015).

$$\begin{aligned}u(x,y,z)&=u_0(x,y)+z\theta_x(x,y)+z^2\psi_x(x,y)+z^3\beta_x(x,y)\\ v(x,y,z)&=v_0(x,y)+z\theta_y(x,y)+z^2\psi_y(x,y)+z^3\beta_y(x,y)\\ w(x,y,z)&=w_0(x,y)\end{aligned} \tag{7}$$

Where, (u, v, w) are the displacement along x, y, z direction. (u_0, v_0, w_0) are the displacement of a point on the mid-plane. θ_x and θ_y is the rotation about x and y axis respectively. ψ_x, ψ_y, β_x and β_y are higher order terms of Taylor series expansion.

3.2 strain-displacement relation

The Nonlinear Green-Lagrange strain-displacement relation for SWCNTRC shell panels is given by (Kar and Panda 2015)

$$\{\varepsilon\}=\begin{Bmatrix}\varepsilon_x\\ \varepsilon_y\\ \gamma_{xy}\\ \gamma_{xz}\\ \gamma_{yz}\end{Bmatrix}=\begin{Bmatrix}\left(\frac{\partial u}{\partial x}+\frac{w}{R_1}\right)\\ \left(\frac{\partial v}{\partial y}+\frac{w}{R_2}\right)\\ \left(\frac{\partial u}{\partial y}+\frac{\partial v}{\partial x}+\frac{2w}{R_1R_2}\right)\\ \left(\frac{\partial u}{\partial z}+\frac{\partial w}{\partial x}-\frac{u}{R_1}\right)\\ \left(\frac{\partial v}{\partial z}+\frac{\partial w}{\partial y}-\frac{v}{R_2}\right)\end{Bmatrix}+\begin{Bmatrix}\frac{1}{2}\left[\left(\frac{\partial u}{\partial x}+\frac{w}{R_1}\right)^2+\left(\frac{\partial v}{\partial x}+\frac{w}{R_1R_2}\right)^2+\left(\frac{\partial w}{\partial x}-\frac{u}{R_1}\right)^2\right]\\ \frac{1}{2}\left[\left(\frac{\partial u}{\partial y}+\frac{w}{R_1R_2}\right)^2+\left(\frac{\partial v}{\partial y}+\frac{w}{R_2}\right)^2+\left(\frac{\partial w}{\partial y}-\frac{v}{R_2}\right)^2\right]\\ \left[\left(\frac{\partial u}{\partial x}+\frac{w}{R_1}\right)\left(\frac{\partial v}{\partial x}+\frac{w}{R_1R_2}\right)+\left(\frac{\partial v}{\partial x}+\frac{w}{R_1R_2}\right)\left(\frac{\partial v}{\partial y}+\frac{w}{R_2}\right)+\left(\frac{\partial w}{\partial x}-\frac{u}{R_1}\right)\left(\frac{\partial w}{\partial y}-\frac{v}{R_2}\right)\right]\\ \left[\frac{\partial u}{\partial z}\left(\frac{\partial u}{\partial x}+\frac{w}{R_1}\right)+\frac{\partial v}{\partial z}\left(\frac{\partial v}{\partial x}+\frac{w}{R_1R_2}\right)+\frac{\partial w}{\partial z}\left(\frac{\partial w}{\partial x}-\frac{u}{R_1}\right)\right]\\ \left[\frac{\partial u}{\partial z}\left(\frac{\partial u}{\partial y}+\frac{w}{R_1R_2}\right)+\frac{\partial v}{\partial z}\left(\frac{\partial v}{\partial y}+\frac{w}{R_2}\right)+\frac{\partial w}{\partial z}\left(\frac{\partial w}{\partial y}-\frac{v}{R_2}\right)\right]\end{Bmatrix} \tag{8}$$

The Eq. (8) can be written as,

$$\begin{aligned}
\varepsilon_x &= \varepsilon_x^0 + \varepsilon_x^4 + z\left(k_x^1 + k_x^5\right) + z^2\left(k_x^2 + k_x^6\right) + z^3\left(k_x^3 + k_x^7\right) + z^4 k_x^8 + z^5 k_x^9 + z^6 k_x^{10} \\
\varepsilon_y &= \varepsilon_y^0 + \varepsilon_y^4 + z\left(k_y^1 + k_y^5\right) + z^2\left(k_y^2 + k_y^6\right) + z^3\left(k_y^3 + k_y^7\right) + z^4 k_y^8 + z^5 k_y^9 + z^6 k_y^{10} \\
\gamma_{xy} &= \varepsilon_{xy}^0 + \varepsilon_{xy}^4 + z\left(k_{xy}^1 + k_{xy}^5\right) + z^2\left(k_{xy}^2 + k_{xy}^6\right) + z^3\left(k_{xy}^3 + k_{xy}^7\right) + z^4 k_{xy}^8 + z^5 k_{xy}^9 + z^6 k_{xy}^{10} \\
\gamma_{xz} &= \varepsilon_{xz}^0 + \varepsilon_{xz}^4 + z\left(k_{xz}^1 + k_{xz}^5\right) + z^2\left(k_{xz}^2 + k_{xz}^6\right) + z^3\left(k_{xz}^3 + k_{xz}^7\right) + z^4 k_{xz}^8 + z^5 k_{xz}^9 + z^6 k_{xz}^{10} \\
\gamma_{yz} &= \varepsilon_{yz}^0 + \varepsilon_{yz}^4 + z\left(k_{yz}^1 + k_{yz}^5\right) + z^2\left(k_{yz}^2 + k_{yz}^6\right) + z^3\left(k_{yz}^3 + k_{yz}^7\right) + z^4 k_{yz}^8 + z^5 k_{yz}^9 + z^6 k_{yz}^{10}
\end{aligned} \tag{9}$$

Total strain vector is sum of linear strain and nonlinear strain vectors can be expressed by

$$\{\varepsilon\} = [T_l]\left\{\overline{\varepsilon(\mathrm{l})}\right\} + [T_{nl}]\left\{\overline{\varepsilon(\mathrm{nl})}\right\} \tag{10}$$

Where,

$$\left\{\overline{\varepsilon(\mathrm{l})}\right\} = \left\{\varepsilon_x^0\ \varepsilon_y^0\ \varepsilon_{xy}^0\ \varepsilon_{xz}^0\ \varepsilon_{yz}^0 k_x^1 k_y^1 k_{xy}^1 k_{xz}^1 k_{yz}^1 k_x^2 k_y^2 k_{xy}^2 k_{xz}^2 k_{yz}^2 k_x^3 k_y^3 k_{xy}^3 k_{xz}^3 k_{yz}^3\right\}^T$$

$$\left\{\overline{\varepsilon(\mathrm{nl})}\right\} = \left\{\varepsilon_x^4\varepsilon_y^4\varepsilon_{xy}^4\varepsilon_{xz}^4\varepsilon_{yz}^4 k_x^5 k_y^5 k_{xy}^5 k_{xz}^5 k_{yz}^5 k_x^6 k_y^6 k_{xy}^6 k_{xz}^6 k_{yz}^6 k_x^7 k_y^7 k_{xy}^7 k_{xz}^7 k_{yz}^7 k_x^8 k_y^8 k_{xy}^8 k_{xz}^8 k_{yz}^8 k_x^9 k_y^9 k_{xy}^9 k_{xz}^9 k_{yz}^9 k_x^{10} k_y^{10} k_{xy}^{10} k_{xz}^{10} k_{yz}^{10}\right\}^T$$

$\left\{\overline{\varepsilon(\mathrm{l})}\right\}$ and $\left\{\overline{\varepsilon(\mathrm{nl})}\right\}$ mid-plane curvature vector for linear and nonlinear respectively, detail all terms are given in appendix-A.

Displacement vector can be defined by

$$\{q\} = \sum_{i=1}^{9} N_i \{q(\mathrm{n})\} \tag{11}$$

$\{q(\mathrm{n})\}$ is the nodal displacements vector at node i. Shape function (N_i) of isoperimetric quadratic nine noded elements (Reddy 2004) can be expressed as

$$\begin{aligned}
&N_1 = \frac{1}{4}\left(\zeta^2 - \zeta\right)\left(\eta^2 - \eta\right); N_2 = \frac{1}{4}\left(\zeta^2 + \zeta\right)\left(\eta^2 - \eta\right)\ ;\ N_3 = \frac{1}{4}\left(\zeta^2 + \zeta\right)\left(\eta^2 + \eta\right); \\
&N_4 = \frac{1}{4}\left(\zeta^2 - \zeta\right)\left(\eta^2 + \eta\right); N_5 = \frac{1}{2}\left(1 - \zeta^2\right)\left(\eta^2 + \eta\right); N_6 = \frac{1}{2}\left(\zeta^2 + \zeta\right)\left(1 - \eta^2\right); \\
&N_7 = \frac{1}{2}\left(1 - \zeta^2\right)\left(\eta^2 + \eta\right)\ ;\ N_8 = \frac{1}{2}\left(\zeta^2 - \zeta\right)\left(1 - \eta^2\right); N_9 = \left(1 - \zeta^2\right)\left(1 - \eta^2\right)
\end{aligned} \tag{12}$$

Mid-plane strain vector for linear and nonlinear can be written as

$$\left\{\overline{\varepsilon(\mathrm{l})}\right\} = [Bq]\{q(\mathrm{n})\} \quad \text{and} \quad \left\{\overline{\varepsilon(\mathrm{nl})}\right\} = [\mathrm{S}][\Omega]\{q(\mathrm{n})\} \tag{13}$$

Where, [Bq], [S] and $[\Omega]$ are linear and nonlinear differential operator matrix respectively, all matrixes are given in Appendix-A.

3.3 Stress and strain relation

Stress and strain relation is given by

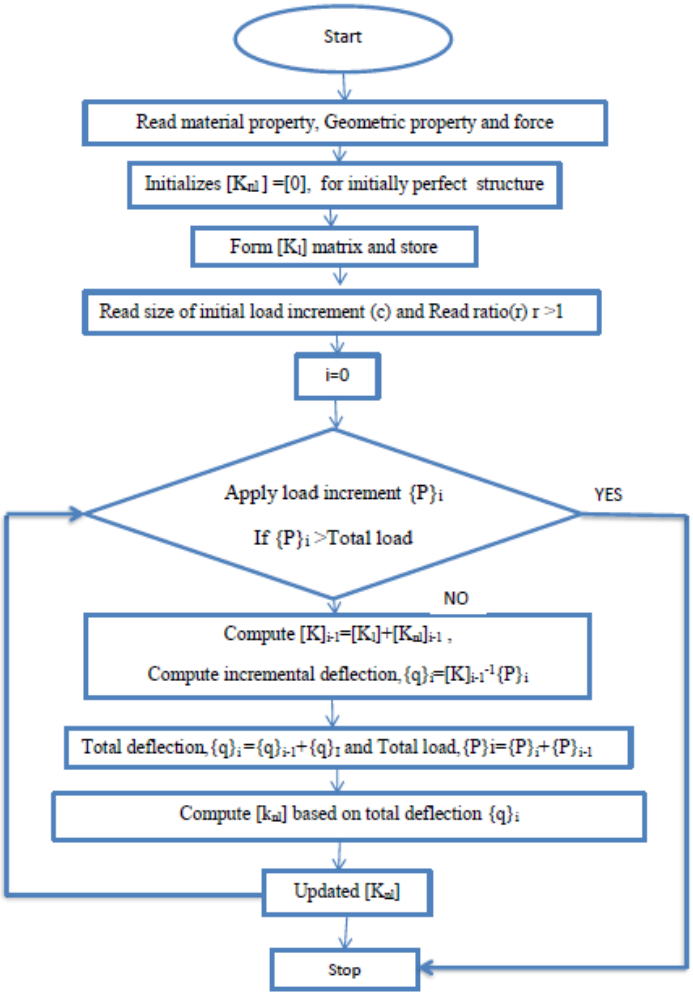

Fig. 4 Flow chart for Newton Raphson Force incrimental Technique

$$\{\sigma\} = \left[\overline{Q}\right]\{\varepsilon\} \tag{14}$$

Where, $\{\sigma\} = \left\{\sigma_x \sigma_y \tau_{xy} \tau_{xz} \tau_{yz}\right\}^T$ and $\{\varepsilon\} = \{\varepsilon_x\ \varepsilon_y\ \gamma_{xy}\ \gamma_{xz}\ \gamma_{yz}\}^T$ are stress and strain vectors respectively. $\left[\overline{Q}\right]$ is the transferred reduced elastic constant matrix.

3.4 The strain energy of the SWCNTRC shell panel

The strain energy of the SWCNTRC shell panel can be defined by,

$$U = \frac{1}{2}\int_A \left[\left\{\overline{\varepsilon(\mathrm{l})}\right\}^T [\mathrm{D}_1]\left\{\overline{\varepsilon(\mathrm{l})}\right\} + \left\{\overline{\varepsilon(\mathrm{l})}\right\}^T [\mathrm{D}_2]\left\{\overline{\varepsilon(\mathrm{nl})}\right\}^T + \left\{\overline{\varepsilon(\mathrm{nl})}\right\}^T [\mathrm{D}_3]\left\{\overline{\varepsilon(\mathrm{nl})}\right\}^T + \left\{\overline{\varepsilon(\mathrm{nl})}\right\}^T [\mathrm{D}_4]\left\{\overline{\varepsilon(\mathrm{l})}\right\}\right] dA \tag{15}$$

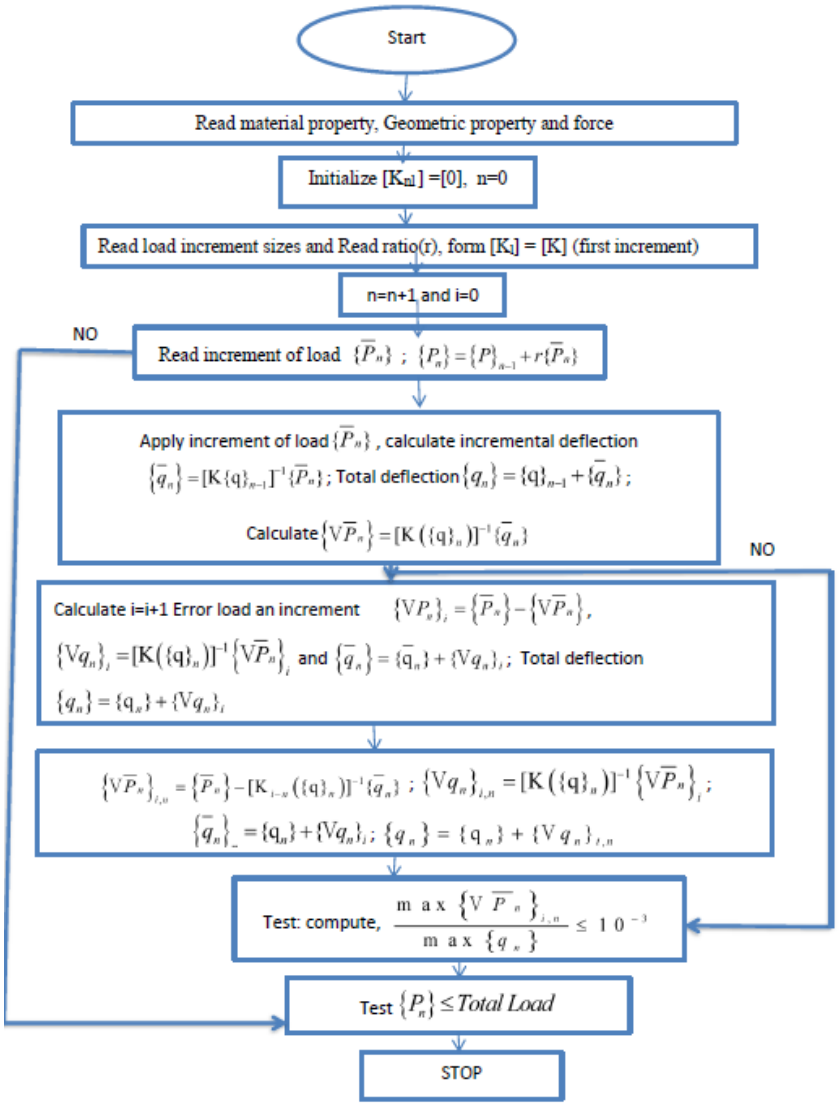

Fig. 5 Flow chart for itration procedure steps

Where, $[D_1]=\int_{-\frac{h}{2}}^{+\frac{h}{2}}[T_l]^T[Q][T_l]^T dz$, $[D_2]=\int_{-\frac{h}{2}}^{+\frac{h}{2}}[T_l]^T[Q][T_{nl}]dz$, $[D_3]=\int_{-\frac{h}{2}}^{+\frac{h}{2}}[T_{nl}]^T[Q][T_l]dz$ and $[D_4]=\int_{-\frac{h}{2}}^{+\frac{h}{2}}[T_{nl}]^T[Q][T_{nl}]dz$.

3.5 Work done of SWCNTRC shell panels due to external loading

The total work done by external Loading (P) is defined by

$$W = \iint \{q(\mathrm{g})\}\{P\}\, dxdy \tag{16}$$

Where, $P = \{00\mathrm{P}000000\}$ is Force vector and $\{q(\mathrm{g})\}$ is global displacement vector.

The total potential energy of SWCNTRC shell panels can be defined by,

$$\prod = U - W \tag{17}$$

Substituting Eqs. (15) and (16) into Eq. (17), we get

$$\frac{\partial \prod}{\partial q(\mathrm{g})} = 0 \tag{18}$$

Solving Eq. (18) we get,

$$[K]\{q(\mathrm{g})\} = \{\mathrm{F}\} \tag{19}$$

Where, $[\mathrm{K}] = [\mathrm{K}_l] + [\mathrm{K}_{nl}]$;

$[\mathrm{K}_l]$ is linear stiffness matrix and $[\mathrm{K}_{nl}]$ is nonlinear stiffness matrix.

4. Solution procedure

The nonlinear bending responses are obtained by using newton Raphson load incremental technique and step iteration flowchart as shown in Figs. 4 and 5 respectively. The detail procedure for obtained nonlinear deflection of SWCNTRC shell panels following steps,

I. First a small displacement solution of the stiffness equation Eq. (19) is obtained for the first load and set $[\mathrm{K}_{nl}] = 0$.

II. The obtained linear deflection substitute in [S] matrix and determine nonlinear stiffness matrix.

III. Total internal resisting force at any nodal for each harmonic is obtained by substituting stored displacement vector in the above step into the linear and nonlinear stiffness equation based on displacement from (II)

IV. The incremental displacement within a load step (i) can be solved.

V. From step no (IV) are added the total displacement and update [Knl] matrix is evaluated.

VI. Convergence Test: in the large deflection (Nonlinear) problem the value has been set at 10^{-3}.

The detail procedure is given Figs. 4-5 and respective equations as follows,

Incremental solution of nonlinear stiffness Equation may be expressed as

$$\{q\}_n = [K]_n^{-1}\{P\}_n + \{q\}_{n-1} \tag{20}$$

$[K_{nl}] = [0]$----for perfect structure

Where, $\{q\}_n$ = total displacement vector at any stage 'n'; $\{P\}_n$ =is the increment in load vectors at n^{th} load step.

$$\left\{\bar{q}_n\right\}=\left[K\left\{q_{n-1}\right\}\right]^{-1},\ \ \left\{q_n\right\}=\left\{q\right\}_{n-1}+\left\{\bar{q}_n\right\} \tag{21}$$

Where, $\left\{\bar{q}_n\right\}$ =deflection due to incremental load $\left\{\overline{P_n}\right\}$. $\left\{q_n\right\}$ =total deflection at any stage, n[th] increment. N,I is increment steps ant cycle respectively.

$$\left\{\nabla\overline{P_n}\right\}_i=\left\{\overline{P}_n\right\}-\left\{\nabla\overline{P_n}\right\};\ \ \left\{\nabla\bar{q}_n\right\}_i=\left[K\left\{q_n\right\}\right]^{-1}\left\{\nabla\overline{P_n}\right\}_i;\left\{q\right\}_n=\left\{q\right\}_n+\left\{\nabla\bar{q}_n\right\}_i \tag{22}$$

Where, $\left\{\nabla\overline{P_n}\right\}_i$ = Error load after cycle (i). $\left\{\nabla\bar{q}_n\right\}_i$ = incremental deflection at cycle (i). $\left\{q\right\}_n$ =Total deflection at any incremental stage (n).

5. Results and discussion

The nonlinear bending analysis of SWCNTRC shell panels are investigated by MATLAB-2013a software code based on the present mathematical model. The present study, The SWCNTRC Shell panels are made of SWCNT and polymer matrix. Here, poly (methyl methacrylate) to as PMMA is considered as the matrix materials. The mechanical properties of PMMA are taken from (Lei *et al.* 2013), E_m=3.52 *Gpa* and ν_m=0.3. SWCNT (10, 10) are chosen as reinforcement material. The SWCNT properties taken from (Dai and Ting 2014), SWCNT (10, 10): (Length=9.26 nm, Diameter =1.36 nm, Thickness= 0.067 nm)

$$E_{11}^{CNT}=103.23GPa, E_{22}^{CNT}=E_{33}^{CNT}=6.05GPa, \mathrm{G}_{12}^{CNT}=2.11GPa, \nu_{12}^{CNT}=\nu_{21}^{CNT}=0.33, \nu_{23}^{CNT}=0.51$$

The elastic properties of SWCNTRC shell panels are calculated from Eq. (6). The elastic properties are substituted in stiffness matrix and compute unknown deflections by using Eq. (26). The nine node isoperimetric elements are considered for present analysis as shown in Fig. 2(a). Non-dimensional transversely uniform distributed load and central deflection are $q_0=\frac{P}{E_m}\left(\frac{a}{h}\right)^4$ and $W_0=\frac{q(\mathrm{g})}{h}$ of SWCNTRC shell panels respectively.

Following boundary condition are employed for nonlinear responses of SWCNTRC shell panels,

a) CCCC

$u_0=v_0=w_0=\theta_x=\theta_y=\psi_x=\psi_y=\beta_x=\beta_y=0$ at X=0, a and y=0,b.

b) CSCS

$v_0=w_0=\theta_y=\psi_y=\beta_y=0$ at x=0, a

$u_0=v_0=w_0=\theta_x=\theta_y=\psi_x=\psi_y=\beta_x=\beta_y=0$ at y=0,b

c) CFFF

$u_0=v_0=w_0=\theta_x=\theta_y=\psi_x=\psi_y=\beta_x=\beta_y=0$ at y=0;

d) SSSS

$u_0=w_0=\theta_y=\psi_y=\beta_y=0$ at x=0,a

$u_0=w_0=\theta_x=\psi_x=\beta_x=0$ at y=0,b

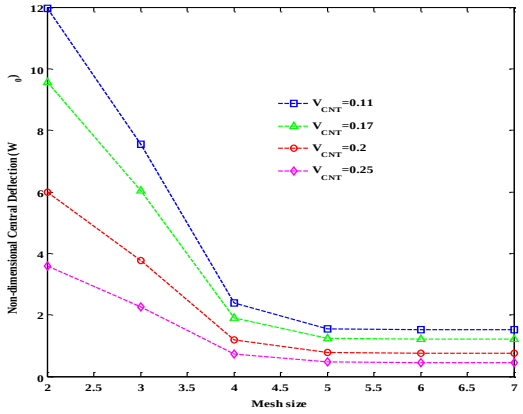

Fig. 6 Convergence behavior of nonlinear deflection of SWCNTRC cylindrical shell panel with a/b=1, a/h= 20, q_0=0.1MPa and R/a=50

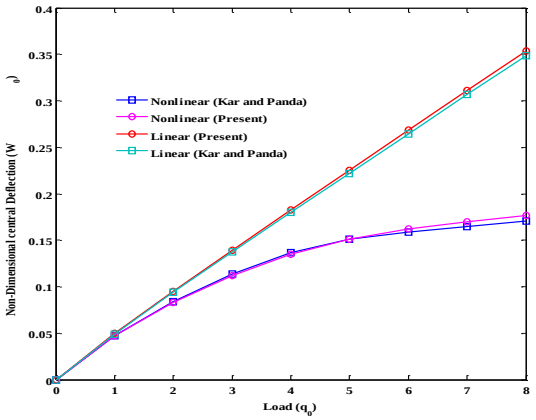

Fig. 7 Linear-Nonlinear non-dimensional central deflection of simply supotred cylindrical shell panel

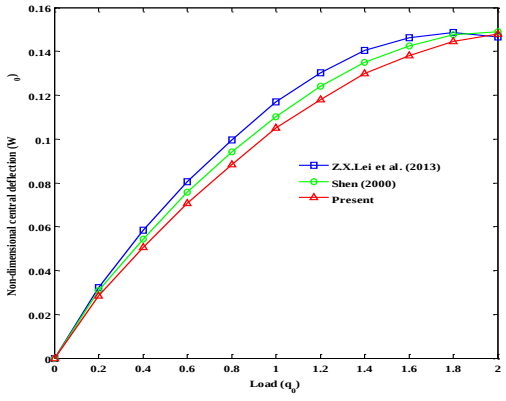

Fig. 8 Nonlinear non-dimensional central deflection of simply supotred flat shell panel

Present nonlinear SWCNTRC shell panels of shape function and regular nodal distribution 5×5 as shown in Fig. 2. The convergence studies is carried out first for nonlinear bending analysis of

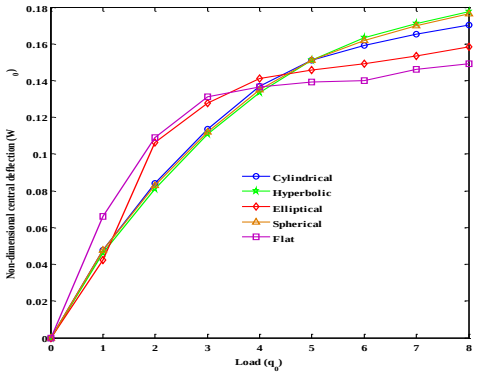

Fig. 9 load and Non-dimensional central deflection for Cylindrical, Hyperbolic, Elliptical, Spherical and Flat shell panel

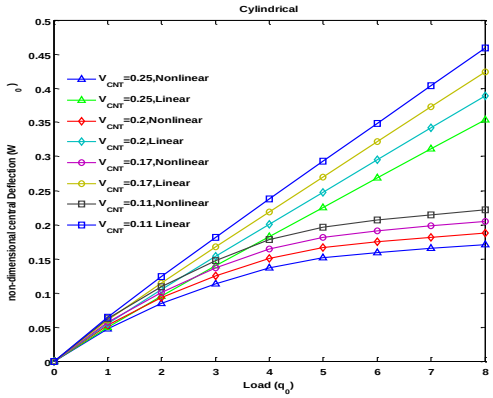

Fig. 10 load and Non-dimensional central deflection of linear and nonlinear for cylindrical shell panel with varying volume fraction of SWCNT

simply supported SWCNTRC shell panel subjected to lateral pressure q_0=0.1 MPa. Non-dimensional nonlinear central deflection and mesh density as shown in Fig. 6. It can be seen that the variation of deflection up to mesh size 5×5, after that deflection are constant of mesh size form 5×5 to 7×7. Therefore, a discretized with 5×5 element is used for all further analysis.

The central deflection (W_0) and non-dimensional load parameter (q_0) of Cylindrical shell panel subjected to a uniform transverse load P=4×10^5 *Pa* with, shell aspect ratio $a/b = 1$, $a/h = 20$, $R/a = 5$ are used to validation purpose. The present results are a compared with the (Kar and Panda 2015) for linear and nonlinear deflection as shown Fig. 7. The present results are in good agreement with (Kar and Panda 2015). Nonlinear bending responses of SWCNTRC shell panel is compared with available literature. The geometric and materials properties of shell panels respectively is given for comparison purpose, a=b=12in and h=0.138in and E_1=3×10^6 *psi*, E_2=1.28×10^6 *psi*, G_{12}=G_{23}=G_{13}=0.37×10^6 *psi*, v_{12}=v_{23}=0.32. Fig. 8 shows nonlinear deflection and load curve of simply supported SWCNTRC flat shell subjected to uniformly distributed loading. The present nonlinear deflection is compared with Lei *et al.* (2013). The present result is in good agreement with Lei *et al.* (2015).

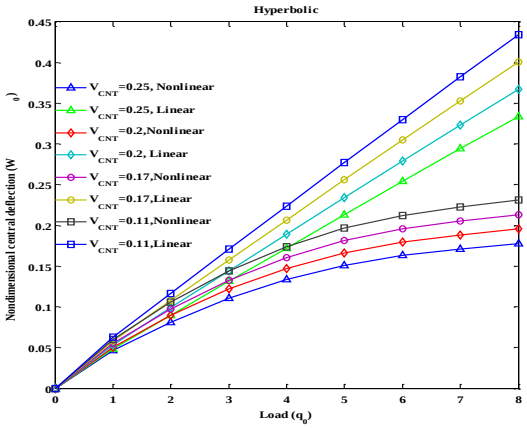

Fig. 11 variation of non-dimensional central deflection of Hyperbolic SWCNTRC shell panel for different volume fraction of SWCNTs

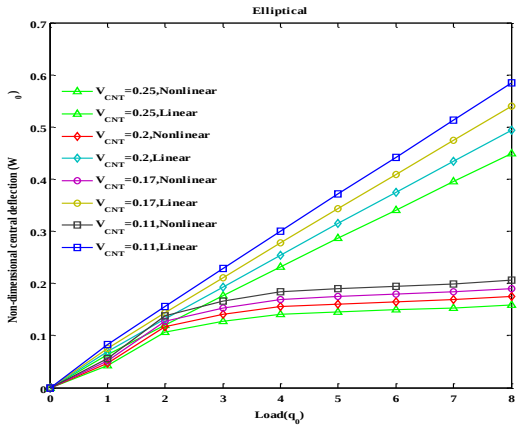

Fig. 12 variation of non-dimensional central deflection of Elliptical SWCNTRC shell panel for different volume fraction of SWCNTs

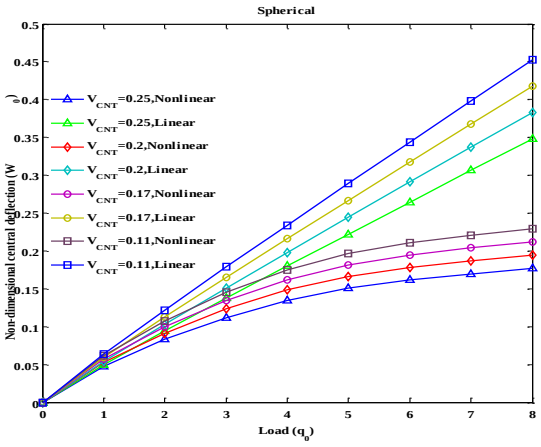

Fig. 13 variation of linear and nonlinear non-dimensional central deflection of Spherical SWCNTRC shell panel for different volume fraction of SWCNTs

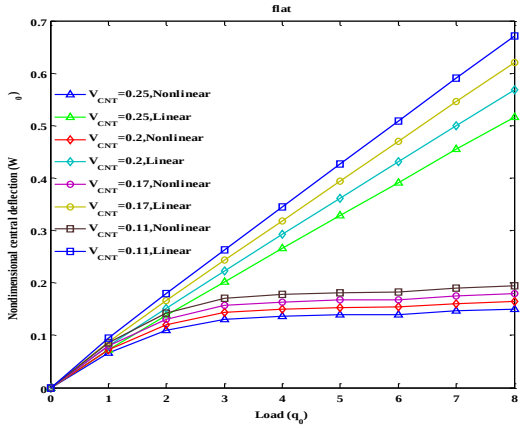

Fig. 14 variation of linear-nonlinear non-dimensional central deflection of Flat SWCNTRC shell panel for different volume fraction of SWCNTs

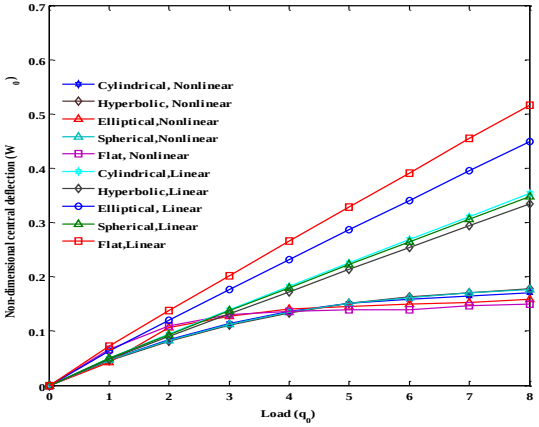

Fig. 15 variation of linear and nonlinear non-dimensional central deflection of Cylindrical, Hyperbolic, Elliptical, spherical and Flat SWCNTRC simply supported shell panels

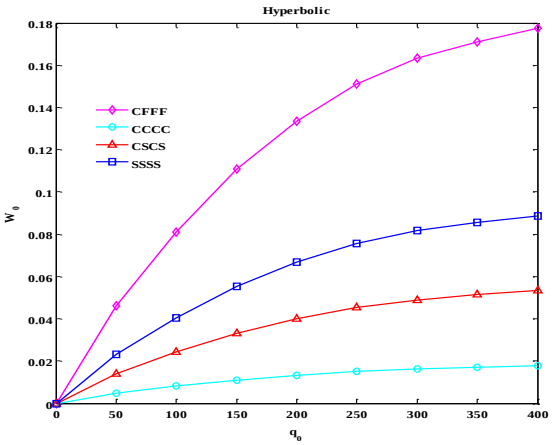

Fig. 16 nonlinear non-dimensional central deflection and load of hyperbolic SWCNTRC shell panels with different boundary condition

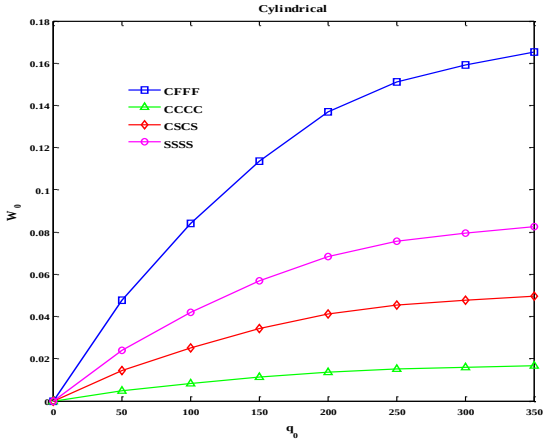

Fig. 17 nonlinear non-dimensional central deflection and load of cylindrical SWCNTRC shell panels with different boundary condition

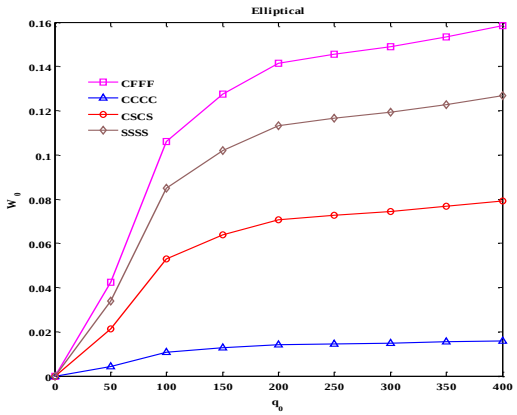

Fig. 18 Nonlinear non-dimensional central deflection and load of Elliptical SWCNTRC shell panels with different boundary condition

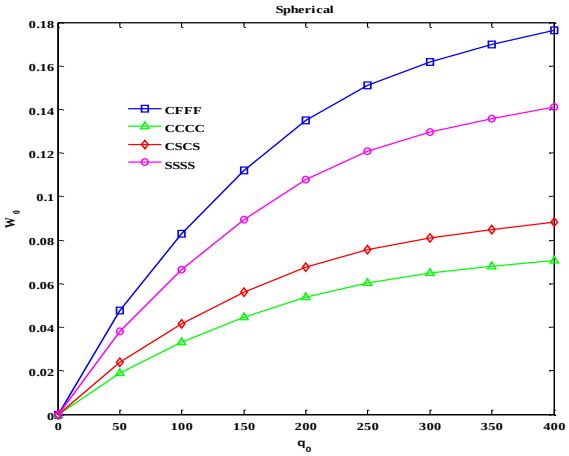

Fig. 19 nonlinear non-dimensional central deflection and load of spherical SWCNTRC shell panels with different boundary condition

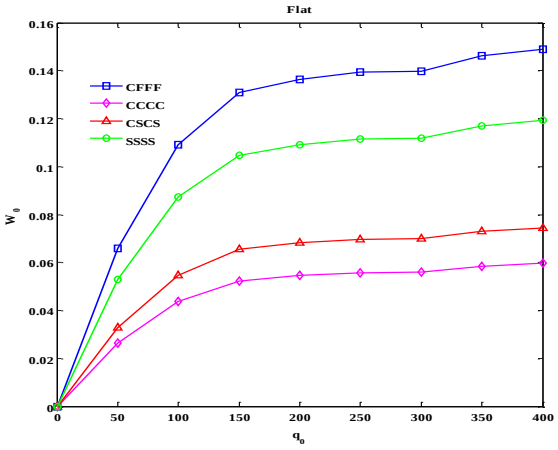

Fig. 20 Nonlinear non-dimensional central deflection and load of flat SWCNTRC shell panels with different boundary condition

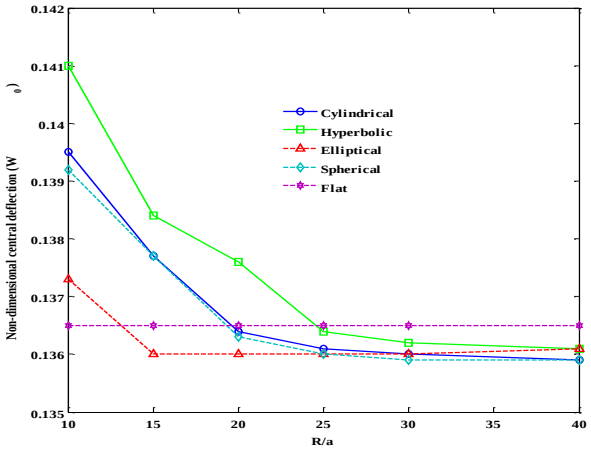

Fig. 21 variation of non-dimensional central deflection of Cylindrical, Hyperbolic, Elliptical, spherical and Flat SWCNTRC simply supported shell panels for different R/a ratio

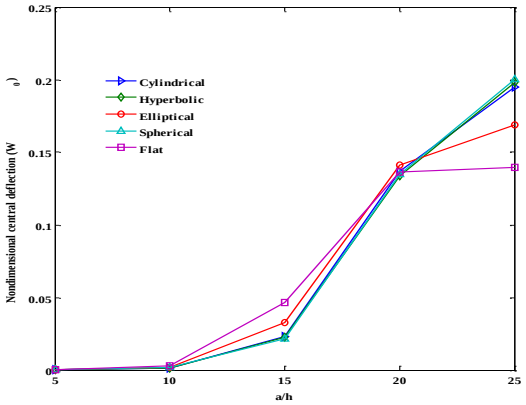

Fig. 22 variation of non-dimensional central deflection of Cylindrical, Hyperbolic, Elliptical, spherical and Flat SWCNTRC simply supported shell panels for different a/h ratio

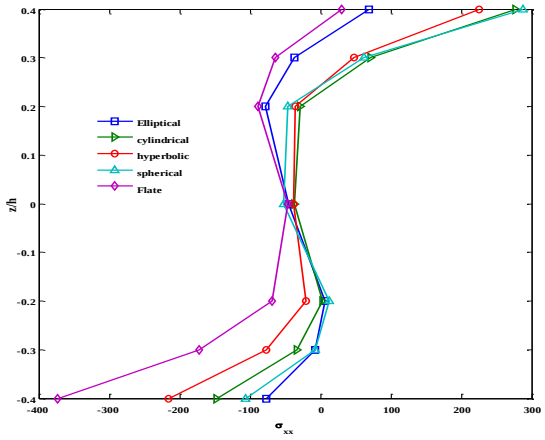

Fig. 23 Through-thickness distributions of non-dimensional normal stresses (σ_{xx}) for Elliptical, Cylindrical, and hyperbolic, spherical and Flat SWCNTRC shell panels with uniformly transversely loading

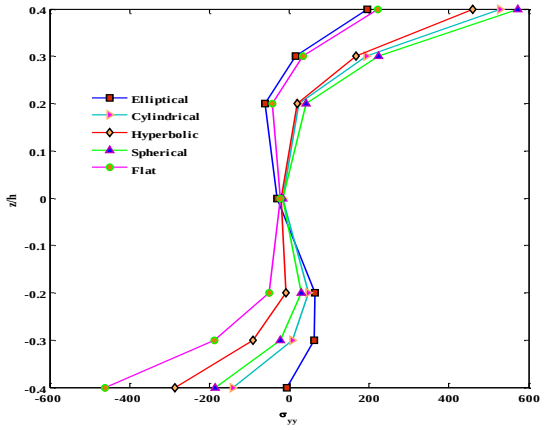

Fig. 24 Through-thickness distributions of non-dimensional normal stresses (σ_{yy}) for Elliptical, Cylindrical, and hyperbolic, spherical and Flat SWCNTRC shell panels with uniformly transversely loading

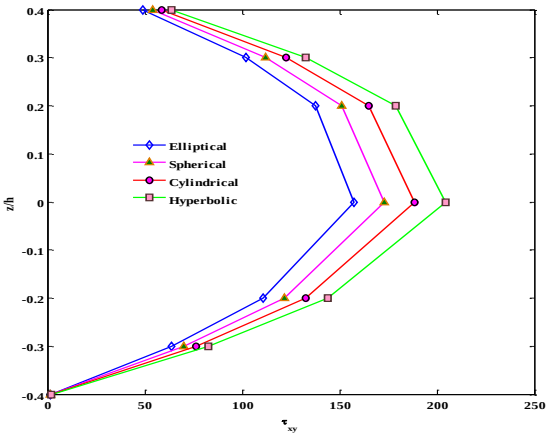

Fig. 25 Through-thickness distributions of shear stresses (τ_{xy}) for Elliptical, Cylindrical, hyperbolic and spherical SWCNTRC shell panels with uniformly transversely loading

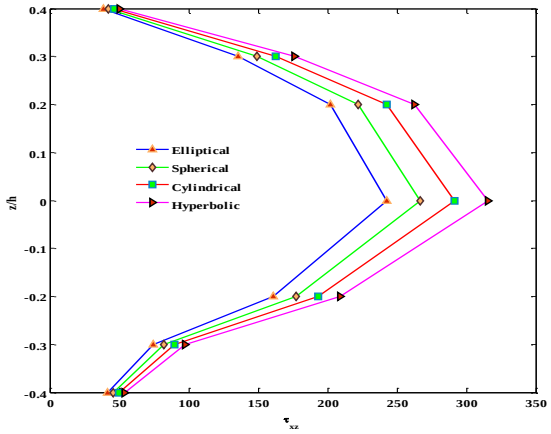

Fig. 26 Through-thickness distributions of shear stresses (τ_{xz}) for Elliptical, Cylindrical, hyperbolic and spherical SWCNTRC shell panels with uniformly transversely loading

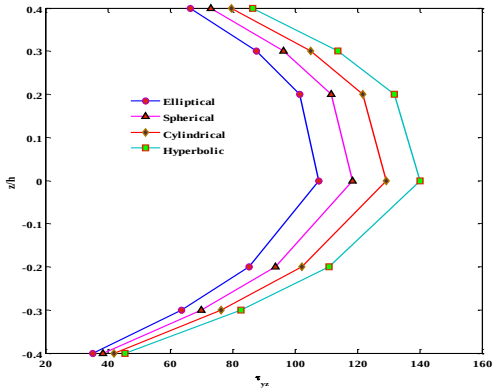

Fig. 27 Through-thickness distributions of shear stresses (τ_{yz}) for Elliptical, Cylindrical, hyperbolic and spherical SWCNTRC shell panels with uniformly transversely loading

Fig. 9 presented nonlinear central deflection and load curves for SWCNTRC shell panels subjected to a uniform transverse load with a/h=20, R/a=5 and V_{CNT}=0.17 simply supported boundary condition. It is observed that the maximum and minimum deflection of hyperbolic and elliptical SWCNTRC shell panels respectively. Fig. 10 depict linear-nonlinear central deflection and load for cylindrical SWCNTRC simply supported shell panels subjected to a uniform transverse load with a/h=20, R/a=5 and V_{CNT}=0.17. It can be seen that the linear and nonlinear non-dimensional central deflection decreased with increasing volume fraction of SWCNT. Fig. 11 shows variation in the linear and nonlinear central deflection of Hyperbolic SWCNTRC shell panel with different volume fraction of SWCNTs. It is observed that maximum deflection of linear as compared to nonlinear deflection of SWCNTRC shell panels. Also, linear-nonlinear deflection of SWCNTRC hyperbolic shell panels decreased with increasing volume fraction of SWCNT. Fig. 12 depicts load and central deflection of linear-nonlinear for elliptical SWCNTRC shell panels subjected to a uniform transverse load with a/h=20, R/a=5 and V_{CNT}=0.17. It can be seen that the linear-nonlinear central deflection decreased with increasing volume fraction of SWCNT. Fig. 13 presents the variation of linear and nonlinear central deflection of spherical SWCNTRC shell panel

with different volume fraction of SWCNTs. It is observed that linear and nonlinear central deflection of SWCNTRC spherical shell panels decreased with increasing volume fraction of SWCNT. Fig. 14 shows linear and nonlinear central deflection and load for flat SWCNTRC shell panels simply supported subjected to a uniform transverse load with a/h=20, R/a=5 and V_{CNT}=0.17. It can be seen that the linear and nonlinear central deflection decreased with increasing volume fraction of SWCNT. Fig. 15 depicts linear and nonlinear central deflection and load of SWCNTRC shell panels subjected to a uniform transverse loading. It can be seen that the maximum and minimum central deflection of Flat and hyperbolic shell panels respectively. Figs. 16-20 shows the load-deflection curves of SWCNTRC hyperbolic, cylindrical, Elliptical, spherical and flat shell panels (a/b=1, a/h=10, R/a=50, V_{CNT}=0.17) under different boundary condition. These results are computed by using CCCC, CSCS, CFFF and SSSS boundary conations. It is observed that nonlinear deflection increased with the increasing load of CFFF boundary condition of SWCNTRC shell panels. However, nonlinear deflection for CCCC boundary condition is lower as compared to other types of boundary conditions. Fig. 21 depicts radius-to-width ratio (R/a) and nonlinear central deflection of SWCNTRC shell panels subjected to a uniform transverse loading with q_0=0.1 MPa, a/h=20 and V_{CNT}=0.17. It can be seen that the nonlinear central deflection of SWCNTRC shell panels decreased with increasing R/a ratio. However flat shell panels are remains constant by changing R/a. Fig. 22 presents width-to-thickness ratio (a/h) and nonlinear central deflection of elliptical SWCNTRC shell panels subjected to a uniform transverse loading with q_0=0.1MPa, R/a=5 and V_{CNT}=0.17. It can be seen that the nonlinear central deflection of SWCNTRC shell panels increased with increasing width-to-thickness ratio. When increases the a/h ratio then shells panels are become thin, so that nonlinear deflection is increased. Fig. 23 non-dimensional normal stress $\sigma_{xx} = \dfrac{\sigma_x h^2}{|q_0| a^2}$ distribution along the non-dimensional thickness (z/h) of Elliptical, Cylindrical, and hyperbolic, spherical and Flat types of SWCNTRC shell panels subjected to a uniform transverse load P=4×10^5 *Pa* with volume fraction V_{CNT}=0.17, shell aspect ratio $a/b = 1$,width thickness ratio , $a/h = 20, R/a = 5$. It can be found that the central normal stress distribution SWCNTRC shell panels are zero at mid-plane and anti-symmetric about the mid-plane due to the symmetric reinforcement with respect to the mid-plane. Fig. 24 non-dimensional normal stress $\sigma_{yy} = \dfrac{\sigma_y h^2}{|q_0| a^2}$ distribution along the non-dimensional thickness (z/h) of Elliptical, Cylindrical, and hyperbolic, spherical and Flat types of SWCNTRC shell panels subjected to a uniform transverse load P=4×10^5 *Pa* with volume fraction V_{CNT}=0.17, shell aspect ratio $a/b = 1$,width thickness ratio , $a/h = 20, R/a = 5$. It can be shown the central normal stress distribution SWCNTRC shell panels are zero at mid-plane and anti-symmetric about the mid-plane due to the symmetric reinforcement with respect to the mid-plane. Fig. 25 non-dimensional Shear stresses ($\tau_{xy} = \dfrac{\tau_{xy} h^2}{|q_0| a^2}$) distribution along the non-dimensional thickness (z/h) of Elliptical, Cylindrical, hyperbolic and spherical types of SWCNTRC shell panels subjected to a uniform transverse load P=4×10^5 *Pa* with volume fraction V_{CNT}=0.17, shell aspect ratio $a/b = 1$,width

thickness ratio , $a/h = 20, R/a = 5$. It can be found that the central shear (τ_{xy}) stress distributions of SWCNTRC shell panels are maximum at mid-plane and symmetric about the mid-plane. Fig. 26 non-dimensional Shear stresses ($\tau_{xz} = \frac{\tau_{xz} h^2}{|q_0| a^2}$) distribution along the non-dimensional thickness (z/h) of Elliptical, Cylindrical, hyperbolic and spherical types of SWCNTRC shell panels subjected to a uniform transverse load P=4×10^5 *Pa* with volume fraction V_{CNT}=0.17, shell aspect ratio $a/b = 1$,width thickness ratio , $a/h = 20, R/a = 5$. It can be seen that the central shear (τ_{xz}) stress distributions of SWCNTRC shell panels are maximum at mid-plane and symmetric about the mid-plane Fig. 27 non-dimensional Shear stresses ($\tau_{yz} = \frac{\tau_{yz} h^2}{|q_0| a^2}$) distribution along the non-dimensional thickness (z/h) of Elliptical, Cylindrical, hyperbolic and spherical types of SWCNTRC shell panels subjected to a uniform transverse load P=4×10^5 *Pa* with volume fraction V_{CNT}=0.17, shell aspect ratio $a/b = 1$,width thickness ratio , $a/h = 20, R/a = 5$. It can be found that the central shear (τ_{xz}) stress distributions of SWCNTRC shell panels are maximum at mid-plane and symmetric about the mid-plane.

6. Conclusions

In this article, the linear-nonlinear bending characteristic of different geometries of SWCNTRC shell panels subjected to uniform lateral loading is investigated. The geometric nonlinear mathematical model of SWCNTRC shell panel is developed on the basis of HSDT kinematics and Green–Lagrange nonlinearity. The effective material properties of SWCNTRC shell panels are estimated by using Eshelby-Mori-Tanaka model. The governing differential equation is derived using the total potential energy principle. The SWCNTRC shell panels are discretized into the nine node isoperimetric elements. The nonlinear bending responses are computed by using a Newton-Raphson method.

Following points are concluded:

• It is observed that the central deflection increased with width-to-thickness increasing of SWCNTRC shell panels.

• The deflection decreased with increasing volume fraction of SWCNT of SWCNTRC shell panels.

• The non-dimensional deflection of Elliptical shell panel is greater than the other types of SWCNTRC panels.

• The Maximum normal stresses (σ_x, σ_y) are presented at top and bottom of SWCNTRC shell panels surface.

• Maximum shear stresses (τ_{xy}, τ_{yz} and τ_{xz}) at mid-plane of SWCNTRC shell panels.

References

Chavan, S.G. and Lal, A. (2017), “Bending behavior of SWCNT reinforced composite plates”, *Steel*

Compos. Struct., **24**(5), 537-548.
Chavan, S.G. and Lal, A. (2017), "Bending analysis of laminated SWCNT reinforced functionally graded plate using FEM", *Curv. Lay. Struct.*, **4**(1), 134-145.
Chavan, S.G. and Lal, A. (2017), "Dynamic bending response of SWCNT reinforced composite plates subjected to hygro-thermo-mechanical loading", *Comput. Concrete*, **20**(2), 229-246.
Dai, H.L. and Dai, T. (2014), "Analysis for the thermo-elastic bending of a functionally graded material cylindrical shell", *Meccan.*, **49**, 1069-1081.
Jin, G., Ye, T., Ma, X., Chen, Y., Su, Z. and Xie, X. (2013), "A unified approach for the vibration analysis of moderately thick composite laminated cylindrical shells with arbitrary boundary conditions", *J. Mech. Sci.*, **75**, 357-376.
Kar, V.R. and Panda, S.K. (2015), "Thermo-elastic analysis of functionally graded doubly curved shell panels using nonlinear finite element method", *Compos. Struct.*, **129**, 202-212.
Katariya, P.V. and Panda, S.K. (2016), "Thermal buckling and vibration analysis of laminated composite curved shell panel", *Aircr. Eng. Aerosp. Technol.*, **88**(1), 97-107.
Khatibinia, M., Feizbakhsh, A., Mohseni, E. and Ranjbar, M.M. (2016), "Modeling mechanical strength of self-compacting mortar containing nanoparticles using wavelet-based support vector machine", *Comput. Concrete*, **18**(6) 1065-1082.
Kulikov, G.M., Mamontov, A.A., Plotnikova, S.V. and Mamontov, S.A. (2016), "Exact geometry solid-shell element based on a sampling surfaces technique for 3D stress analysis of doubly-curved composite shells", *Curv. Lay. Struct.*, **3**(1), 1-16.
Lal, A., Singh, B.N. and Anand, S. (2011), "Nonlinear bending response of laminated composite spherical shell panel with system randomness subjected to hygro-thermo-mechanical loading", *J. Mech. Sci.*, **53**, 855-866.
Lei, Z.X., Liew, K.M. and Yu, J.L. (2013), "Large deflection analysis of functional graded carbon nanotube-reinforcement composite plates by element-free Kp-ritz method", *Comput. Meth. Appl. Mech. Eng.*, **256**, 189-199.
Lezgy-Nazargah, M. and Cheraghi, N. (2015), "An exact peano series solution for bending analysis of imperfect layered FG neutral magneto-electro-elastic plates resting on elastic foundations", *Mech. Adv. Mater. Struct.*, **24**(3), 183-199.
Lopatin, A., Morozov, E.V. and Shatov A.V. (2016), "Bending of the composite lattice cylindrical shell with the midspan rigid disk loaded by transverse inertia forces", *Compos. Struct.*, **150**, 181-190.
Mahapatra Trupti, R., Kar Vishesh, R. and Panda, S.K. (2015), "Nonlinear free vibration analysis of laminated composite doubly curved shell panel in hygro-thermal environment", *J. Sandw. Struct. Mater.*, 1-35.
Mahapatra, T.R., Mehar, K., Panda, S.K., Dewangan, S. and Dash, S. (2016), "Flexural strength of functionally graded nanotube reinforced sandwich spherical panel", *Mater. Sci. Eng.*, 178 012031.
Mehar, K. and Panda, S.K. (2015), "Free vibration and bending behaviour of CNT reinforced composite plate using different shear deformation theory", *Mater. Sci. Eng.*, **115**(1), 012014.
Mehar, K., Panda, S.K. (2016), "Geometrical nonlinear free vibration analysis of FG-CNT reinforced composite flat panel under uniform thermal field", *Compos. Struct.*, **143**, 336-346.
Mehar, K. and Panda, S.K. (2016), "Nonlinear static behaviors of FG-CNT reinforced composite flat panel under thermo-mechanical load", *J. Aerosp. Eng.*, **30**(3), 04016100.
Mehar, K. and Panda, S.K. (2016), "Numerical investigation of nonlinear thermom-echanical deflection of functionally graded CNT reinforced doubly curved composite shell panel under different mechanical loads", *Compos. Struct.*, **161**, 287-298.
Mehar, K. and Panda, S.K. (2016), "Thermal free vibration behaviour of FG-CNT reinforced sandwich curved panel using finite element method", *Polym. Compos.*
Mehar, K., Panda, S.K., Dehengia, A. and Kar, V.R. (2015), "Vibration analysis of functionally graded carbon nanotube reinforced composite plate in thermal environment", *J. Sandw. Struct. Mater.*, **18**(2), 151-173.
Orakdogen, E., Kuçukarslan, S., Sofiyev, A. and Omurtag, M.H. (2010), "Finite element analysis of

functionally graded plates for coupling effect of extension and bending", *Meccan*., **45**, 63-72.
Orakdogen, E., Kuçukarslan, S., Sofiyev, A. and Omurtag, M.H. (2010), "Finite element analysis of functionally graded plates for coupling effect of extension and bending", *Meccan*., **45**, 63-72.
Panda, S.K. and Singh, B.N. (2009), "Nonlinear free vibration of spherical shell panel using higher order shear deformation theory-a finite element approach", *J. Press. Vess. Pip*., **86**, 373-383.
Panda, S.K. and Singh, B.N. (2009), "Nonlinear free vibration of spherical shell panel using higher order shear deformation theory-a finite element approach", *J. Press. Vess. Pip*., **86**, 373-383.
Reddy, J.N. (2004), *Mechanics of Laminated Composite Plate and Shells*, 2nd Edition, CRC Press, New York, Washington, U.S.A.
Sadowski, A.J. and Michael, R.J. (2013), "Solid or shell finite elements to model thick cylindrical tubes and shells under global bending", *J. Mech. Sci*., **74**, 143-153.
Shariyat, M. (2012), "A general nonlinear global-local theory for bending and buckling analyses of imperfect cylindrical laminated and sandwich shells under thermo-mechanical loads", *Meccan*., **47**, 301-319.
Shen, H.S. and Xiang, Y. (2014), "Nonlinear bending of nanotube-reinforced composite cylindrical panels resting on elastic foundations in thermal environments", *Eng. Struct*., **80**, 163-172.
Sobhani, A.B., Nasrollah, B.A.H. and Hedayati, H. (2012), "Eshelby-Mori-Tanaka approach for vibrational behavior of continuously graded carbon nanotube-reinforced cylindrical panels", *Compos. Part B*, **43**, 1943-1954.
Sofiyev, A.H., Karaca, Z. and Zerin, Z. (2017), "Non-linear vibration of composite orthotropic cylindrical shells on the non-linear elastic foundations within the shear deformation theory", *Compos. Struct*., **159**, 53-62.
Song, Z.G., Zhang, L.W. and Liew, K.M. (2016), "Vibration analysis of CNT-reinforced functionally graded composite cylindrical shells in thermal environments", *J. Mech. Sci*., **115**, 339-347.
Tornabene, F. and Viola, E. (2009), "Free vibration analysis of functionally graded panels and shells of revolution", *Meccan*., **44**, 255-281.

EC

Nomenclature and abbreviation

E_{11}, E_{22} and E_{33}	Young's modulus of the composite shell panels
v_{12}, v_{21}	Poison's ratio of composite material
$E_{11}^{CNT}, E_{22}^{CNT}, E_{33}^{CNT}$	Young's modulus of SWCNTs
$G_{12}^{CNT}, G_{23}^{CNT}$ *and* $v_{12}^{CNT}, v_{21}^{CNT}, v_{23}^{CNT}$	Shear modulus and poison's ratio of SWCNTs
E_m and v_m	Young's modulus and poison's ratio of matrix
V_{CNT} and V_m	Effective volume fraction of SWCNT and matrix
W_{CNT}, ρ_{CNT} and ρ_m	Mass fraction, Density of SWCNT and density of matrix
k_{CNT}, l_{CNT}, n_{CNT}, m_{CNT} and p_{CNT}	Hill elastic constant of SWCNT

a, b, h	Shell panel length, width and thickness
R_1 and R_2	Principle curvature radii
W_0	Non-dimensional central deflection
SWCNT	Single Wall Carbon Nanotube
SWCNTRC	Single Wall Carbon Nanotube Reinforced Composite

Appendix A

Linear Thickness coordinate matrix $[T_l]$

$$[T_l]=\begin{bmatrix}
1&0&0&0&0&z&0&0&0&0&z^2&0&0&0&0&z^3&0&0&0&0\\
0&1&0&0&0&0&z&0&0&0&0&z^2&0&0&0&0&z^3&0&0&0\\
0&0&1&0&0&0&0&z&0&0&0&0&z^2&0&0&0&0&z^3&0&0\\
0&0&0&1&0&0&0&0&z&0&0&0&0&z^2&0&0&0&0&z^3&0\\
0&0&0&0&1&0&0&0&0&z&0&0&0&0&z^2&0&0&0&0&z^3
\end{bmatrix}$$

Non-Linear Thickness coordinate matrix $[T_{nl}]$

$$[T_{nl}]=\begin{bmatrix}
1&0&0&0&0&z&0&0&0&0&z^2&0&0&0&0&z^3&0&0&0&0\\
0&1&0&0&0&0&z&0&0&0&0&z^2&0&0&0&0&z^3&0&0&0\\
0&0&1&0&0&0&0&z&0&0&0&0&z^2&0&0&0&0&z^3&0&0\\
0&0&0&1&0&0&0&0&z&0&0&0&0&z^2&0&0&0&0&z^3&0\\
0&0&0&0&1&0&0&0&0&z&0&0&0&0&z^2&0&0&0&0&z^3
\end{bmatrix}\ldots$$

$$\begin{bmatrix}
z^4&0&0&0&0&z^5&0&0&0&0&z^6&0&0\\
0&z^4&0&0&0&0&z^5&0&0&0&0&z^6&0\\
0&0&z^4&0&0&0&0&z^5&0&0&0&0&z^6\\
0&0&0&z^4&0&0&0&0&z^5&0&0&0&0\\
0&0&0&0&z^4&0&0&0&0&z^5&0&0&0
\end{bmatrix}$$

$$[\bar{Q}]=\begin{bmatrix}
\bar{Q}_{11}&\bar{Q}_{12}&\bar{Q}_{16}&0&0\\
\bar{Q}_{12}&\bar{Q}_{22}&\bar{Q}_{26}&0&0\\
\bar{Q}_{16}&\bar{Q}_{26}&\bar{Q}_{66}&0&0\\
0&0&0&\bar{Q}_{44}&\bar{Q}_{45}\\
0&0&0&\bar{Q}_{45}&\bar{Q}_{55}
\end{bmatrix}$$

Individual terms of matrix [Bq]

$$[Bq]_{1,1}=\frac{\partial}{\partial x}\ ;\quad [Bq]_{1,3}=\frac{1}{R_1}\ ;\quad [Bq]_{2,2}=\frac{\partial}{\partial y}\ ;\ [Bq]_{2,3}=\frac{1}{R_2}\quad [Bq]_{3,1}=\frac{\partial}{\partial y}\ ;\ [Bq]_{3,2}=\frac{\partial}{\partial x}\quad ;$$

$$[Bq]_{3,3}=\frac{2}{R_1R_2};\ [Bq]_{4,1}=-\frac{1}{R_1};[Bq]_{4,3}=\frac{\partial}{\partial x}\ ;[Bq]_{4,4}=1\ ;[Bq]_{5,2}=-\frac{1}{R_2}\ ;[Bq]_{5,3}=\frac{\partial}{\partial x};$$

$$[Bq]_{5,5}=1 \;;\; [Bq]_{6,4}=\frac{\partial}{\partial x} \;;\; [Bq]_{7,5}=\frac{\partial}{\partial y} \;;\; [Bq]_{8,4}=\frac{\partial}{\partial y} \;;\; [Bq]_{8,5}=\frac{\partial}{\partial x} \;;\; [Bq]_{9,4}=-\frac{1}{R_1} \;;$$

$$[Bq]_{9,6}=2 \;;\; [Bq]_{10,5}=-\frac{1}{R_2} \;;\; [Bq]_{10,7}=2 \;;\; [Bq]_{11,6}=\frac{\partial}{\partial x} \;;\; [Bq]_{12,7}=\frac{\partial}{\partial y} \;;\; [Bq]_{13,6}=\frac{\partial}{\partial y} \;;$$

$$[Bq]_{13,7}=\frac{\partial}{\partial x} \;;\; [Bq]_{14,7}=-\frac{1}{R_1} \;;\; [Bq]_{14,8}=2 \;;\; [Bq]_{15,7}=-\frac{1}{R_2} \;;\; [Bq]_{15,9}=2 \;;\; [Bq]_{16,8}=\frac{\partial}{\partial x} \;;$$

$$[Bq]_{17,9}=\frac{\partial}{\partial y};[Bq]_{18,8}=\frac{\partial}{\partial y};[Bq]_{18,9}=\frac{\partial}{\partial x};[Bq]_{19,8}=-\frac{1}{R_1};[Bq]_{20,9}=-\frac{1}{R_2}$$

Linear Mid-plane strain terms

$$\varepsilon_x^0=\frac{\partial u}{\partial x} \;;\; \varepsilon_y^0=\frac{\partial v}{\partial y};\; \varepsilon_{xy}^0=\frac{\partial u}{\partial y}+\frac{\partial v}{\partial x};\; \varepsilon_{xz}^0=\frac{\partial w}{\partial x}+\theta_x;\; \varepsilon_{yz}^0=\frac{\partial w}{\partial y}+\theta_y;\; k_x^1=\frac{\partial \theta_x}{\partial x};\; k_y^1=\frac{\partial \theta_y}{\partial y};$$

$$k_{xy}^1=\frac{\partial \theta_x}{\partial y}+\frac{\partial \theta_y}{\partial x} \;;\; k_{xz}^1=\psi_x-\frac{\theta_x}{R_1} \;;\; k_{yz}^1=2\psi_y-\frac{\theta_y}{R_2} \;;\; k_x^2=\frac{\partial \psi_x}{\partial x} \;;\; k_y^2=\frac{\partial \psi_y}{\partial y} \;;$$

$$k_{xy}^2=\frac{\partial \psi_x}{\partial y}+\frac{\partial \psi_y}{\partial x} \;;\; k_{xz}^2=2\beta_x-\frac{\psi_x}{R_1} \;;\; k_{yz}^2=2\beta_y-\frac{\psi_y}{R_2} \;;\; k_x^3=\frac{\partial \beta_x}{\partial x} \;;\; k_y^3=\frac{\partial \beta_y}{\partial y} \;;$$

$$k_{xy}^3=\frac{\partial \beta_x}{\partial y}+\frac{\partial \beta_y}{\partial x};\; k_{xz}^3=-\frac{\beta_x}{R_1};\; k_{yz}^3=-\frac{\beta_y}{R_2}$$

Non-linear mid-plane strain terms

$$\varepsilon_x^4=\frac{1}{2}\frac{\partial^2 u}{\partial x^2}+\frac{1}{2}\frac{\partial^2 v}{\partial x^2}+\frac{1}{2}\frac{\partial^2 w}{\partial x^2};\quad \varepsilon_y^4=\frac{1}{2}\frac{\partial^2 u}{\partial y^2}+\frac{1}{2}\frac{\partial^2 v}{\partial y^2}+\frac{1}{2}\frac{\partial^2 w}{\partial y^2} \;;\; \varepsilon_{xy}^4=\frac{\partial^2 u}{\partial x\partial y}+\frac{\partial^2 v}{\partial x\partial y}+\frac{\partial^2 w}{\partial x\partial y}$$

$$\varepsilon_{xz}^4=\frac{\partial u}{\partial x}\frac{\partial \theta_x}{\partial x}+\frac{\partial v}{\partial x}\frac{\partial \theta_y}{\partial x} \;;\; \varepsilon_{yz}^4=\frac{\partial u}{\partial y}\theta_x+\frac{\partial v}{\partial y}\theta_y \;;\; k_x^5=\frac{\partial u}{\partial x}\frac{\partial \theta_x}{\partial x}+\frac{\partial v}{\partial x}\frac{\partial \theta_y}{\partial x}-\frac{\partial w}{\partial x}\frac{\theta_x}{R_1} \;;$$

$$k_y^5=\frac{\partial u}{\partial x}\frac{\partial \theta_x}{\partial y}+\frac{\partial v}{\partial y}\frac{\partial \theta_y}{\partial y}-\frac{\partial w}{\partial y}\frac{\theta_y}{R_2} \;;$$

$$k_{xy}^5=\frac{\partial u}{\partial x}\frac{\partial \theta_x}{\partial y}+\frac{\partial u}{\partial y}\frac{\partial \theta_y}{\partial x}+\frac{\partial v}{\partial x}\frac{\partial \theta_y}{\partial y}+\frac{\partial v}{\partial y}\frac{\partial \theta_x}{\partial y}-\frac{\partial w}{\partial x}\frac{\theta_y}{R_2}-\frac{\partial w}{\partial y}\frac{\theta_x}{R_1} \;;$$

$$k_{xz}^5=2\frac{\partial u}{\partial x}\psi_x+2\frac{\partial v}{\partial x}\psi_y+\frac{\partial \theta_x}{\partial x}\theta_x+\frac{\partial \theta_y}{\partial y}\theta_y \;;\; k_{yz}^5=2\frac{\partial u}{\partial y}\psi_x+2\frac{\partial v}{\partial y}\psi_y-\frac{\partial \theta_x}{\partial x}\theta_x+\frac{\partial \theta_y}{\partial y}\theta_y$$

$$k_{yz}^5=2\frac{\partial u}{\partial y}\psi_x+2\frac{\partial v}{\partial y}\psi_y-\frac{\partial \theta_x}{\partial x}\theta_x+\frac{\partial \theta_y}{\partial y}\theta_y$$

$$k_x^6=\frac{\partial u}{\partial x}\frac{\partial \psi_x}{\partial x}+\frac{\partial v}{\partial x}\frac{\partial \psi_x}{\partial x}-\frac{\partial w}{\partial x}\frac{\psi_x}{R_1}+\frac{1}{2}\frac{\partial^2 \theta_x}{\partial x^2}+\frac{1}{2}\frac{\partial^2 \theta_x}{\partial y^2}+\frac{1}{2}\frac{\partial^2 \theta_x}{\partial x^2}\frac{\psi_x}{R_1^2}$$

$$k_y^6 = \frac{\partial u}{\partial y} + \frac{\partial v}{\partial y}\frac{\partial \psi_y}{\partial y} - \frac{\partial w}{\partial y}\frac{\psi_y}{R_2} + \frac{1}{2}\frac{\partial^2 \theta_x}{\partial y^2} + \frac{1}{2}\frac{\partial^2 \theta_y}{\partial y^2} + \frac{1}{2}\frac{\theta_y^2}{R_1^2}$$

$$k_{xy}^6 = \frac{\partial u}{\partial x}\frac{\partial \psi_x}{\partial x} + \frac{\partial u}{\partial y}\frac{\partial \psi_x}{\partial x} + \frac{\partial v}{\partial x}\frac{\partial \psi_y}{\partial y} + \frac{\partial v}{\partial y}\frac{\partial \psi_x}{\partial x} - \frac{\partial w}{\partial x}\frac{\psi_x}{R_1} - \frac{\partial w}{\partial y}\frac{\psi_x}{R_1} + \frac{\partial \theta_x}{\partial x}\frac{\partial \theta_x}{\partial y} + \frac{\partial \theta_y}{\partial x}\frac{\partial \theta_x}{\partial y} + \frac{\theta_x \theta_y}{R_1 R_2}$$

$$k_{xz}^6 = 3\frac{\partial u}{\partial x}\beta_x + 3\frac{\partial v}{\partial y}\beta_y + 2\frac{\partial \theta_x}{\partial y}\psi_x + 2\frac{\partial \theta_y}{\partial x}\psi_y + \frac{\partial \psi_x}{\partial x}\theta_x + \frac{\partial \psi_y}{\partial x}\theta_y$$

$$k_{yz}^6 = 3\frac{\partial u}{\partial y}\beta_x + 3\frac{\partial v}{\partial y}\beta_y + 2\frac{\partial \theta_x}{\partial y}\psi_x + 2\frac{\partial \theta_y}{\partial y}\psi_y + \frac{\partial \psi_x}{\partial y}\theta_x + \frac{\partial \psi_y}{\partial y}\theta_y$$

$$k_x^7 = \frac{\partial u}{\partial x}\frac{\partial \beta_x}{\partial x} + \frac{\partial v}{\partial x}\frac{\partial \beta_y}{\partial x} - \frac{\partial w}{\partial x}\frac{\beta_x}{R_1} + \frac{\partial \theta_x}{\partial x}\frac{\partial \psi_x}{\partial x} + \frac{\partial \theta_y}{\partial x}\frac{\partial \psi_y}{\partial x} + \theta_x\frac{\psi_x}{R_1^2}$$

$$k_y^7 = \frac{\partial u}{\partial y}\frac{\partial \beta_x}{\partial y} + \frac{\partial v}{\partial y}\frac{\partial \beta_y}{\partial y} - \frac{\partial w}{\partial y}\frac{\beta_y}{R_1} + \frac{\partial \theta_x}{\partial y}\frac{\partial \psi_x}{\partial y} + \frac{\partial \theta_y}{\partial y}\frac{\partial \psi_y}{\partial y} + \theta_x\frac{\psi_x}{R_2^2}$$

$$k_{xy}^7 = \frac{\partial u}{\partial x}\frac{\partial \beta_x}{\partial y} + \frac{\partial u}{\partial y}\frac{\partial \beta_x}{\partial x} + \frac{\partial v}{\partial x}\frac{\partial \beta_y}{\partial y} + \frac{\partial v}{\partial y}\frac{\partial \beta_y}{\partial x} - \frac{\partial w}{\partial x}\frac{\beta_y}{R_2} - \frac{\partial w}{\partial y}\frac{\beta_x}{R_1} + \frac{\partial \psi_y}{\partial y}\frac{\partial \theta_x}{\partial x} + \frac{\partial \theta_x}{\partial y}\frac{\partial \psi_x}{\partial x} + \frac{\partial \theta_y}{\partial x}\frac{\partial \psi_y}{\partial y} + \frac{\partial \theta_y}{\partial y}\frac{\partial \psi_y}{\partial x} + \frac{\theta_x \psi_y}{R_1 R_2} + \frac{\theta_y \psi_x}{R_1 R_2}$$

$$k_{xz}^7 = 3\frac{\partial \theta_x}{\partial x}\beta_x + 3\frac{\partial \theta_y}{\partial x}\beta_y + 2\frac{\partial \psi_x}{\partial x}\psi_x + 2\frac{\partial \psi_y}{\partial x}\psi_y + \frac{\partial \beta_x}{\partial x}\theta_x + \frac{\partial \beta_y}{\partial x}\theta_y$$

$$k_{yz}^7 = 3\frac{\partial \theta_x}{\partial y}\beta_x + 3\frac{\partial \theta_y}{\partial y}\beta_y + 2\frac{\partial \psi_x}{\partial y}\psi_x + 2\frac{\partial \psi_y}{\partial y}\psi_y + \frac{\partial \beta_x}{\partial y}\theta_x + \frac{\partial \beta_y}{\partial y}\theta_y$$

$$k_x^8 = \frac{\partial \theta_x}{\partial x}\frac{\partial \beta_x}{\partial x} + \frac{\partial \theta_y}{\partial x}\frac{\partial \beta_y}{\partial x} + \frac{1}{2}\left(\frac{\partial \psi_x}{\partial x}\right)^2 + \frac{1}{2}\left(\frac{\partial \psi_y}{\partial x}\right)^2 + \theta_x\frac{\psi_x}{R_1^2} + \frac{1}{2}\left(\frac{\psi_x}{R_1}\right)^2$$

$$k_y^8 = \frac{\partial \theta_x}{\partial y}\frac{\partial \beta_x}{\partial y} + \frac{\partial \theta_y}{\partial y}\frac{\partial \beta_y}{\partial y} + \frac{1}{2}\left(\frac{\partial \psi_x}{\partial y}\right)^2 + \frac{1}{2}\left(\frac{\partial \psi_y}{\partial y}\right)^2 + \theta_x\frac{\psi_y}{R_2^2} + \frac{1}{2}\left(\frac{\psi_y}{R_2}\right)^2$$

$$k_{xy}^8 = \frac{\partial \theta_x}{\partial x}\frac{\partial \beta_x}{\partial y} + \frac{\partial \theta_x}{\partial y}\frac{\partial \beta_y}{\partial x} + \frac{\partial \theta_y}{\partial x}\frac{\partial \beta_x}{\partial y} + \frac{\partial \theta_y}{\partial y}\frac{\partial \beta_y}{\partial x} - \frac{\partial \psi_x}{\partial x}\frac{\partial \psi_x}{\partial y} + \frac{\partial \psi_y}{\partial x}\frac{\partial \beta_y}{\partial y} + \frac{\theta_x \beta_y}{R_1 R_2} + \frac{\theta_y \beta_y}{R_1 R_2} + \frac{\psi_x \psi_y}{R_1 R_2}$$

$$k_{xz}^8 = 3\frac{\partial \psi_x}{\partial x}\beta_x + 3\frac{\partial \beta_x}{\partial x}\beta_y + 2\frac{\partial \beta_x}{\partial x}\psi_x + 2\frac{\partial \chi_y}{\partial x}\psi_y$$

$$k_{yz}^8 = 3\frac{\partial \psi_x}{\partial y}\beta_x + 3\frac{\partial \beta_x}{\partial y}\beta_y + 2\frac{\partial \beta_x}{\partial y}\psi_x + 2\frac{\partial \chi_y}{\partial y}\psi_y$$

$$k_x^9 = \frac{\partial \psi_x}{\partial x}\frac{\partial \beta_x}{\partial x} + \frac{\partial \psi_y}{\partial x}\frac{\partial \beta_y}{\partial x} + \frac{\beta_x \psi_x}{R_1^2} \quad ; \quad k_x^9 = \frac{\partial \psi_x}{\partial y}\frac{\partial \beta_x}{\partial y} + \frac{\partial \psi_y}{\partial y}\frac{\partial \beta_y}{\partial y} + \frac{\beta_x \psi_x}{R_2^2}$$

$$k_{xy}^{9}=\frac{\partial\psi_x}{\partial x}\frac{\partial\beta_x}{\partial y}+\frac{\partial\psi_x}{\partial y}\frac{\partial\beta_x}{\partial x}+\frac{\partial\psi_y}{\partial y}\frac{\partial\beta_y}{\partial x}+\frac{\psi_x\beta_y}{R_1R_2}+\frac{\psi_y\beta_x}{R_1R_2}\qquad k_{xz}^{9}=3\frac{\partial\beta_x}{\partial y}\beta_x+3\frac{\partial\theta_y}{\partial x}\beta_y\quad ;$$

$$k_{yz}^{9}=3\frac{\partial\beta_x}{\partial y}\beta_x+3\frac{\partial\beta_y}{\partial x}\beta_y\quad ;\qquad k_{x}^{10}=\frac{1}{2}\left(\frac{\partial\beta_x}{\partial x}\right)^2+\frac{1}{2}\left(\frac{\partial\beta_y}{\partial x}\right)^2+\frac{1}{2}\left(\frac{\beta_x}{R_1}\right)^2\quad ;$$

$$k_{y}^{10}=\frac{1}{2}\left(\frac{\partial\beta_x}{\partial y}\right)^2+\frac{1}{2}\left(\frac{\partial\beta_y}{\partial y}\right)^2+\frac{1}{2}\left(\frac{\beta_y}{R_2}\right)^2\quad ;\quad k_{xy}^{10}=\frac{\partial\beta_x}{\partial x}\frac{\partial\beta_x}{\partial y}+\frac{\partial\beta_y}{\partial x}\frac{\partial\beta_y}{\partial y}+\frac{\beta_y\beta_x}{R_1R_2}$$

Individual terms of matrix $[\Omega]$

$$[\Omega]_{1,1}=\frac{\partial}{\partial x}\quad ;\quad [\Omega]_{1,3}=\frac{1}{R_1}\quad ;\quad [\Omega]_{2,1}=\frac{\partial}{\partial y}\quad ;\quad [\Omega]_{2,3}=\frac{1}{R_1R_2}\quad ;\quad [\Omega]_{3,2}=\frac{\partial}{\partial x}\quad ;\quad [\Omega]_{33}=\frac{2}{R_1R_2}\quad ;$$

$$[\Omega]_{4,1}=\frac{1}{R_1R_2}\quad [\Omega]_{4,2}=\frac{\partial}{\partial y}\quad ;\quad [\Omega]_{4,3}=\frac{1}{R_1R_2}\quad ;\quad [\Omega]_{5,1}=-\frac{1}{R_1}\quad ;\quad [\Omega]_{5,3}=\frac{\partial}{\partial x}\quad ;\quad [\Omega]_{6,2}=-\frac{1}{R_2}$$

$$[\Omega]_{6,3}=\frac{\partial}{\partial y};[\Omega]_{7,4}=\frac{\partial}{\partial x};[\Omega]_{8,4}=\frac{\partial}{\partial y};[\Omega]_{9,5}=\frac{\partial}{\partial x};[\Omega]_{10,5}=\frac{\partial}{\partial y};[\Omega]_{11,6}=\frac{\partial}{\partial x};[\Omega]_{12,6}=\frac{\partial}{\partial y};$$

$$[\Omega]_{13,7}=\frac{\partial}{\partial x};[\Omega]_{14,7}=\frac{\partial}{\partial y};[\Omega]_{15,8}=\frac{\partial}{\partial x};[\Omega]_{16,8}=\frac{\partial}{\partial y}\quad [\Omega]_{17,9}=\frac{\partial}{\partial x};[\Omega]_{18,9}=\frac{\partial}{\partial y};[\Omega]_{19,4}=1\ ;$$

$$[\Omega]_{20,5}=1\ ;[\Omega]_{21,6}=1;[\Omega]_{22,7}=1;[\Omega]_{23,8}=1\ ;[\Omega]_{24,9}=1\ .$$

Individual terms of matrix [S]

$$[S]_{1,1}=\frac{1}{2}\frac{\partial u}{\partial x}\ ;\ [S]_{1,3}=\frac{1}{2}\frac{\partial v}{\partial x}\ ;\quad [S]_{1,5}=\frac{1}{2}\frac{\partial w}{\partial x}\ ;\ [S]_{2,2}=\frac{1}{2}\frac{\partial u}{\partial y}\ ;\ [S]_{2,4}=\frac{1}{2}\frac{\partial v}{\partial y}\ ;\ [S]_{2,6}=\frac{1}{2}\frac{\partial w}{\partial y}\ ;$$

$$[S]_{3,1}=\frac{\partial u}{\partial y}\ ;\ [S]_{3,3}=\frac{\partial v}{\partial y}\ ;\ [S]_{3,5}=\frac{\partial w}{\partial y}\ ;\ [S]_{4,1}=\theta_x\ ;\quad [S]_{4,3}=\theta_y\ ;\quad [S]_{5,2}=\theta_x\ ;\ [S]_{5,4}=\theta_y\ ;$$

$$[S]_{6,1}=\frac{\partial\theta_x}{\partial x}\ ;\ [S]_{6,3}=\frac{\partial\theta_y}{\partial x}\ ;\quad [S]_{6,5}=-\frac{\theta_x}{R_1}\ ;\ [S]_{7,2}=\frac{\partial\theta_x}{\partial y}\ ;\ [S]_{7,4}=\frac{\partial\theta_y}{\partial y}\ ;\ [S]_{7,6}=\frac{\theta_y}{R_2}\ ;$$

$$[S]_{8,1}=\frac{\partial\theta_x}{\partial y}\ ;\ [S]_{8,2}=\frac{\partial\theta_x}{\partial x}\ ;\ [S]_{8,3}=\frac{\partial\theta_y}{\partial y}\ ;\ [S]_{8,4}=\frac{\partial\theta_y}{\partial x}\ ;\ [S]_{8,5}=-\frac{\theta_y}{R_2}\ ;\ [S]_{8,6}=-\frac{\theta_x}{R_1}\ ;$$

$$[S]_{9,1}=2\psi_x\ ;[S]_{9,3}=2\psi_y\ ;[S]_{9,7}=\theta_x\ ;[S]_{9,9}=\theta_y\ ;[S]_{10,2}=2\psi_x\ ;[S]_{10,4}=2\psi_y\ ;[S]_{10,8}=\theta_x\ ;$$

$$[S]_{10,10}=\theta_y\ ;\ [S]_{11,1}=\frac{\partial\psi_x}{\partial x}\quad [S]_{11,1}=\frac{\partial\psi_x}{\partial x}\ ;\ [S]_{11,3}=\frac{\partial\psi_y}{\partial x}\ ;\ [S]_{11,5}=-\frac{\psi_x}{R_1}\ ;\ [S]_{11,7}=\frac{1}{2}\frac{\partial\theta_x}{\partial x}\ ;$$

$$[S]_{11,9}=\frac{1}{2}\frac{\partial\theta_y}{\partial x};[S]_{12,2}=\frac{\partial\psi_x}{\partial y};[S]_{12,4}=\frac{\partial\psi_y}{\partial y};[S]_{12,6}=-\frac{\psi_y}{R_2};[S]_{12,8}=\frac{1}{2}\frac{\partial\theta_x}{\partial y};[S]_{12,10}=\frac{1}{2}\frac{\partial\theta_y}{\partial y};$$

$$[S]_{13,1}=\frac{\partial\psi_x}{\partial y}\quad ;\quad [S]_{13,2}=\frac{\partial\psi_x}{\partial x}\quad ;\quad [S]_{13,3}=\frac{\partial\psi_y}{\partial y}\quad ;\quad [S]_{13,4}=\frac{\partial\psi_y}{\partial x}\quad ;\quad [S]_{13,5}=-\frac{1}{2}\frac{\psi_y}{R_2}\quad ;$$

$[S]_{13,6} = -\frac{1}{2}\frac{\psi_x}{R_1}$; $[S]_{13,7} = \frac{\partial \theta_x}{\partial y}$; $[S]_{13,8} = \frac{\partial \theta_y}{\partial y}$; $[S]_{14,1} = 3\beta_x$; $[S]_{14,3} = 3\beta_y$; $[S]_{14,7} = 2\psi_x$;

$[S]_{14,9} = 2\psi_y$; $[S]_{14,11} = \theta_y$; $[S]_{14,13} = \theta_x$; $[S]_{15,2} = 3\beta_y$ $[S]_{15,4} = 3\beta_x$; $[S]_{15,8} = 2\psi_x$;

$[S]_{15,10} = 2\psi_y$; $[S]_{15,12} = \theta_x$; $[S]_{15,14} = \theta_y$; $[S]_{16,1} = \frac{\partial \beta_x}{\partial x}$; $[S]_{16,3} = \frac{\partial \beta_y}{\partial x}$; $[S]_{16,5} = \frac{\beta_x}{R_1}$;

$[S]_{16,7} = \frac{\partial \psi_x}{\partial x}$; $[S]_{16,9} = \frac{\partial \psi_y}{\partial x}$; $[S]_{16,19} = \frac{\beta_x}{R_1^2}$; $[S]_{17,2} = \frac{\partial \beta_x}{\partial y}$; $[S]_{17,4} = \frac{\partial \beta_y}{\partial y}$; $[S]_{17,6} = -\frac{\beta_y}{R_2}$;

$[S]_{17,8} = \frac{\partial \psi_x}{\partial y}$; $[S]_{17,10} = \frac{\partial \psi_y}{\partial y}$; $[S]_{17,20} = -\frac{\psi_y}{R_2^2}$; $[S]_{18,1} = \frac{\partial \beta_x}{\partial y}$; $[S]_{18,2} = \frac{\partial \beta_x}{\partial x}$; $[S]_{18,3} = \frac{\partial \beta_y}{\partial y}$;

$[S]_{18,4} = \frac{\partial \beta_y}{\partial x}$; $[S]_{18,5} = -\frac{\beta_y}{R_2}$; $[S]_{18,6} = -\frac{\beta_x}{R_1}$; $[S]_{18,7} = \frac{\partial \psi_x}{\partial y}$; $[S]_{18,8} = \frac{\partial \psi_x}{\partial x}$; $[S]_{18,9} = \frac{\partial \psi_y}{\partial y}$;

$[S]_{18,10} = \frac{\partial \psi_y}{\partial x}$; $[S]_{18,19} = \frac{\psi_y}{R_1 R_2}$; $[S]_{18,20} = \frac{\psi_x}{R_1 R_2}$; $[S]_{19,7} = 3\beta_y$; $[S]_{19,9} = 3\beta_x$; $[S]_{19,11} = 2\psi_x$;

$[S]_{19,13} = 2\psi_y$; $[S]_{19,15} = \theta_x$; $[S]_{19,17} = \theta_y$; $[S]_{20,8} = 3\beta_x$; $[S]_{20,10} = 3\beta_y$; $[S]_{20,12} = 2\psi_x$;

$[S]_{20,14} = 2\psi_y$; $[S]_{20,16} = \theta_x$; $[S]_{20,18} = \theta_y$; $[S]_{21,7} = \frac{\partial \beta_x}{\partial x}$; $[S]_{21,9} = \frac{\partial \beta_y}{\partial x}$; $[S]_{21,11} = \frac{1}{2}\frac{\partial \psi_x}{\partial x}$;

$[S]_{21,13} = \frac{1}{2}\frac{\partial \psi_y}{\partial x}$; $[S]_{21,19} = \frac{\beta_x}{R_1^2}$; $[S]_{21,21} = \frac{1}{2}\frac{\psi_x}{R_1^2}$; $[S]_{22,8} = \frac{\partial \beta_x}{\partial y}$; $[S]_{22,10} = \frac{\partial \beta_y}{\partial y}$; $[S]_{22,12} = \frac{1}{2}\frac{\partial \psi_x}{\partial y}$;

$[S]_{22,14} = \frac{1}{2}\frac{\partial \psi_y}{\partial y}$; $[S]_{22,20} = \frac{\beta_y}{R_2^2}$; $[S]_{22,22} = \frac{1}{2}\frac{\psi_y}{R_2^2}$; $[S]_{23,7} = \frac{\partial \beta_x}{\partial y}$ $[S]_{23,8} = \frac{\partial \beta_x}{\partial x}$; $[S]_{23,9} = \frac{\partial \beta_y}{\partial y}$;

$[S]_{23,10} = \frac{\partial \beta_y}{\partial x}$; $[S]_{23,11} = \frac{\partial \psi_x}{\partial y}$; $[S]_{23,13} = \frac{\partial \psi_y}{\partial y}$; $[S]_{23,19} = \frac{\beta_y}{R_1 R_2}$; $[S]_{23,20} = \frac{\beta_x}{R_1 R_2}$;

$[S]_{23,21} = \frac{\psi_y}{R_1 R_2}$; $[S]_{24,11} = 3\beta_x$; $[S]_{24,13} = 3\beta_y$; $[S]_{24,15} = 2\psi_x$; $[S]_{24,17} = 2\psi_y$; $[S]_{25,12} = 3\beta_x$;

$[S]_{25,14} = 3\beta_y$; $[S]_{25,16} = 2\psi_x$; $[S]_{25,18} = 2\psi_y$; $[S]_{26,11} = \frac{\partial \beta_x}{\partial x}$; $[S]_{26,13} = \frac{\partial \beta_y}{\partial x}$; $[S]_{26,21} = \frac{\beta_x}{R_1^2}$;

$[S]_{27,12} = \frac{\partial \beta_x}{\partial y}$; $[S]_{27,14} = \frac{\partial \beta_y}{\partial y}$; $[S]_{27,22} = \frac{\beta_y}{R_2^2}$; $[S]_{28,11} = \frac{\partial \beta_x}{\partial y}$; $[S]_{28,12} = \frac{\partial \beta_x}{\partial x}$; $[S]_{28,13} = \frac{\partial \beta_y}{\partial y}$;

$[S]_{28,14} = \frac{\partial \beta_y}{\partial x}$; $[S]_{28,21} = \frac{\beta_y}{R_1 R_2}$; $[S]_{28,22} = \frac{\beta_x}{R_1 R_2}$; $[S]_{29,15} = 3\beta_x$; $[S]_{29,17} = 3\beta_y$; $[S]_{30,16} = 3\beta_x$;

$$[S]_{30,18}=3\beta_y \;\; ; \;\; [S]_{31,15}=\frac{1}{2}\frac{\partial\beta_x}{\partial x} \;\; ; \;\; [S]_{31,17}=\frac{1}{2}\frac{\partial\beta_y}{\partial x} \;\; ; \;\; [S]_{31,23}=\frac{1}{2}\frac{\beta_x}{R_1^2} \;\; ; \;\; [S]_{32,16}=\frac{1}{2}\frac{\partial\beta_x}{\partial y} \;\; ;$$

$$[S]_{32,18}=\frac{1}{2}\frac{\partial\beta_y}{\partial y};[S]_{32,24}=\frac{1}{2}\frac{\beta_y}{R_2^2};[S]_{33,15}=\frac{\partial\beta_x}{\partial y};[S]_{33,17}=\frac{\partial\beta_y}{\partial y};[S]_{33,23}=\frac{\beta_y}{R_1 R_2}$$